IPPJ-AM-54

FINAL (n, 4) STATE-RESOLVED ELECTRON CAPTURE BY MULTIPLY CHARGED IONS FROM NEUTRAL ATOMS

N. SHIMAKURA, N. TOSHIMA, T. WATANABE
AND H. TAWARA

INSTITUTE OF PLASMA PHYSICS
NAGOYA UNIVERSITY

NAGOYA, JAPAN

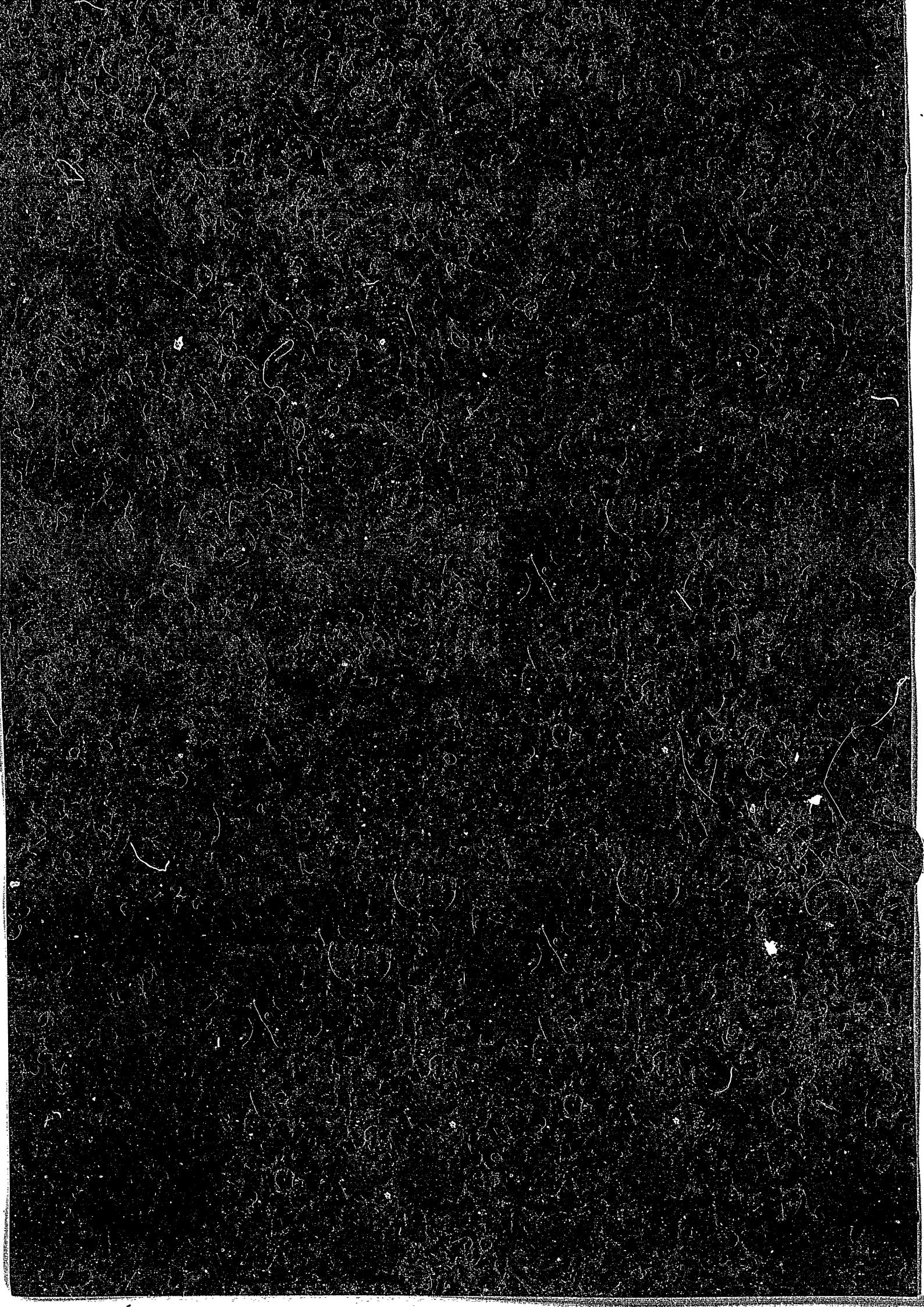

IPPJ-AM-54

FINAL (n, ℓ) STATE-RESOLVED ELECTRON CAPTURE BY MULTIPLY CHARGED IONS FROM NEUTRAL ATOMS

N. Shimakura[1], N. Toshima[2], T. Watanabe[3] and H. Tawara

Institute of Plasma Physics, Nagoya University
Chikusa-ku, Nagoya 464, Japan

August 1987

Permanent Address:
1) Department of General Education, Niigata University, Niigata 950-21
2) Institute of Applied Physics, University of Tsukuba, Sakura-mura, Ibaraki 305
3) The Institute of Physical and Chemical Research (RIKEN), Wako-shi, Saitama 351-01

Abstract

Thanks to the recent development of experimental techniques, it has become possible to measure the cross sections of the final (n, ℓ) state-resolved electron capture processes. As for the process of electron capture by incident multicharged ions from neutral atoms, many theoretical calculations have been made using several different methods, for example, impact parameter methods using molecular basis wavefunctions, or using atomic basis wavefunctions, classical trajectory Monte Carlo method. In this Article a review on the theoretical calculations for the process is given. A particular attention is paid to the difference of the theoretical methods applied for the physics governed in the process, for the selective properties of the capture process and for the absolute values of cross sections from the practical point of view.

1. Introduction

The electron capture process, often called charge transfer process, is one of the major problems in atomic collision physics. The main theoretical difficulty in treating this process arises from the situation that the unperturbed Hamiltonian of the system is changed before and after the collision. The difficulty of such rearrangement collisions is actually solved by taking into consideration practical situation and by taking proper approximations for actual problems. Considering that the colliding system in the initial and final states consist of two incoming and two outgoing particles with some structures, respectively, and these particles are much heavier than the transferred particles (electron), the trajectories of the colliding heavy particles are mainly determined by the two-body (ion-atom) interactions and is not influenced by the electron transfer process itself. This situation makes it possible to treat the problems using the approximations that divide the process into the following two parts; 1) relative motion of the colliding particles and 2) their internal motion of the respective colliding particles. Almost all the methods used to treat the process are approximated basically by this concept; i.e., because of the magnitude of their masses, compared with electron mass, the relative motion follows almost the straight line trajectory or slightly curved trajectory in classical mechanical terminology, or plane-wave or slightly distorted-wave in quantum mechanical terminology. In high velocity collisions this situation allows us to formulate the problem using the straight-line impact parameter approximation or plane-wave Born approximation, meanwhile, in low velocity collisions, it can make the adiabatic approximation useful in solving the problem.

Let us consider the following electron capture process by a bare ion from a neutral atom, i.e.,

$$A^{q+} + B \rightarrow A^{(q-1)+}(n, \ell) + B^{+} \qquad (1\text{-}1)$$

where (n, ℓ) means a particular hydrogen-like atomic state with the principal quantum number n and the angular momentum quantum number ℓ. Experimentally the final atomic state or the final ionic state can be determined by one of two methods, i.e., ion-energy spectroscopy or photon spectroscopy. If an electron is captured from B atom to A^{q+} ion resulting in the $A^{(q-1)+}(n, \ell)$ state, the kinetic energy of $A^{(q-1)+}$ ion is determined in order to satisfy the conservation law of the total energy. Through measurements of the kinetic energy of $A^{(q-1)+}$ ion, we can determine the particular (n,ℓ) state (ion-energy loss/gain spectroscopy). If the final state (n,ℓ) of the electron-captured ion in eq. (1-1) is the optically allowed excited state, the ion can emit a photon through the process:

$$A^{(q-1)+}(n, \ell) \rightarrow A^{(q-1)+}(n', \ell') + h\nu \qquad (1\text{-}2)$$

that can be analyzed by X-ray, UV or visible light photon spectroscopy. Owing to the degeneracy of the energy levels of hydrogen-like ion in the same principal quantum number n, it is difficult to discriminate the angular momentum states by the translational ion energy spectroscopy. Optical measurement can only be made in the case of the allowed excited states and the accurate measurements of the absolute emission intensities are not easy. Thus, both types of the experiments play a complementary role with each other.

When the excited state (n,ℓ) is in autoionizing state, the ion can emit an electron by the process

$$A^{(q-1)+}(n,\ell) \rightarrow A^{q+}(n',\ell') + e. \qquad (1\text{-}3)$$

By the measurement of kinetic energy of the electron, one can obtain the cross section for this process.

For low velocity collision, the cross sections are determined mainly by the level crossing points of potential energy curves. Accordingly the magnitude of cross sections and their behaviour as a function of the incident velocities are quite case-dependent and the electron capture processes are considered to occur selectively into a particular (n, ℓ) state. On the other hand, in high velocity collisions, the cross sections are determined mainly by the overlap of the momentum distributions between the initial and final states of the electron to be transferred. They can be treated universally and some unified treatments are proposed to produce the scaling relationship among various combinations of the colliding systems. The cross section decreases rapidly with the increase of the velocity. The final (n, ℓ) states after electron capture become non-selective and they distributes over a broad range of n and ℓ. This can be interpreted that in high velocity collisions the collision time Δt becomes short and from the relationship of the uncertainty principle between the time and energy, the system can transfer to the state with the energy difference $\hbar/\Delta t$.

One of the most important facts in discussion of the final ℓ-state distribution of electron capture process is the effect of the long range interaction between ions after collision. Following the electron transfer process from a neutral atom to an excited state of multicharged ion shown in eq. (1-1), the energy levels of $A^{(q-1)+}(n, \ell)$ ions are nearly degenerate with

those of many angular momentum states of ℓ. If we expand the interatomic perturbation Hamiltonian in terms of the multipole interaction, the monopole-charge and transition-dipole ineteraction term is of the lowest order of the interaction which can change the electronic state of $A^{(q-1)+}(n, \ell)$. The interaction can be written by

$$\langle n, \ell \,|\Sigma\xi_i|\, n, \ell' \rangle \; R^{-2} \qquad (1\text{-}4)$$

where R is the internuclear distance between the bare ion and the neutral atom, ξ_i (= x_i, y_i or z_i) the component of the Cartesian coordinate of the i-th electron centered at the nucleus of $A^{(q-1)+}$ ion. Due to the long range property of the interaction ($\propto R^{-2}$), the state-changing process from (n, ℓ) to (n, ℓ') is important and can not be ignored. In the case of the fine structure transitions in collisions with rare gas atom such as

$$K(4^2P_{1/2}) + He \rightarrow K(4^2P_{3/2}) + He, \qquad (1\text{-}5)$$

the cross section is of the order of 100 $\mathring{A}^2$. Considering that the interaction is of short-range in a transition-dipole and induced dipole interaction, compared with that in the present case of the charge transfer, the cross sections relevant to the transition can be 10^3 $\mathring{A}^2$ or more. In this sense, the role of the electron translation factor (ETF) is very important to avoid spurious interactions which appear in the matrix elements with the same center in the usual treatment.

In this Report, firstly we introduce and discuss some simple models for the electron capture process such as the classical over-barrier model (COBM or OBM), Landau-Zener model. Then we describe the classical trajectory Monte Carlo (CTMC) method where the colliding particles and an electron are treated

in the completely classical mechanical way. The quantum mechanical probability for finding the system in some particular state which can be determined under the quantum mechanical condition is replaced by the classical statistical probability to find the system in the states which is distributed uniformly in phase space under a given quantum mechanical condition. The uniform distribution is obtained by taking physical quantities using the randomization procedure (Monte Carlo method). Then, as one of typical theoretical techniques, the impact parameter method with atomic basis and that with molecular basis is introduced and discussed. Further, to check the agreement, some compiled data of the cross sections for the final state-resolved electron capture processes by experiments and by theoretical calculations are compared. In the last chapter, the summary and discussion are given. Atomic units are used throughout this article unless otherwise specified.

2. Simple model

Among many theoretical methods for calculating the cross section of the electron capture from a neutral atom by multi-charged ion, the close-coupling method provides the most reliable values if we use sufficient time and labor. However, with increasing the ionic charge and complexity of the electronic structure of the collision system, the application of the close-coupling method encounters considerable practical difficulties. While the simple models such as the over barrier model (OBM) and the multichannel Landau-Zener model (LZM) do not need much time and effort, they can provide the qualitatively reliable values of the cross sections and are useful to obtain the general trend of the cross section behavior.

2.1 Over barrier model

Some different versions of the over-barrier models (OBM) have been proposed and applied to electron capture process. In this section, firstly the OBM proposed by Grozdanov[1] is described and, then, the one by Ryufuku et al[2]. is explained briefly.

Under the adiabatic approximation, Grozdanov treated the motion of electron in the electron capture process from one-electron species by fully stripped ions as motion of fluid of non-interacting classical particles in the field of two Coulomb centers of charges Z_1 and Z_2. The electron capture is considered as the events in which the classical particles go through surface F. The motion of the classical particles is governed by the Hamilton-Jacobi equation and the continuity equation:

$$\partial S/\partial t + H = 0 \qquad (2\text{-}1)$$

$$\partial f/\partial t + \nabla(f\nabla S/m) = 0 \qquad (2\text{-}2)$$

where S is the classical principal function of Hamiltonian, H is the classical Hamilton function, $p = \nabla S$ is the momentum of the classical particle, m is the mass of the particle and f is the spatial probability density. Introducing the prolate spheroidal coordinates (ξ, η, ϕ) and separating the variables in equation (2-1), the solution for the classical principle function S is obtained. This solution involves two kinds of one-dimensional momenta, $p(\xi)$ and $p(\eta)$, which are separated completely. It should be noted that the potential experienced by the electron is also separated into two one-dimensional potentials, one ($V(\xi)$) is along the ξ coordinate and the other ($V(\eta)$) is along the η coordinate. Knowing the solution for the classical principle function and with the help of the separation of the variables again, the spatial probability density is obtained from equation (2-2).

The obtained formula has been applied to the electron capture where an electron in the ground state of hydrogen atom (Z_1=1) is captured into the bare ion (Z_2=Z). The electron energy E and the separation constant λ necessary for the calculation of the transition probability are obtained from the equation of the quantum mechanical asymptotic expansion:

$$E = -1/2 - Z/R \qquad (2\text{-}3)$$

$$\lambda = ZR \qquad (2\text{-}4)$$

where R is the distance between the bare ion and proton. The classically allowed region for the motion of the electron is bound by two kinds of two

turning points $\xi_{1,2}$ and $\eta_{1,2}$, where the momenta of the electron for one-dimensional motions along the ξ and η coordinates, $p(\xi)$ and $p(\eta)$, are zero, respectively. Initially the two allowed regions are separated and belong to the bare ion and proton, respectively. The electron capture becomes possible by the overlappiong of these regions. Here $\eta_{1,2}$ are more important than $\xi_{1,2}$ for the electron capture process. Substituting equations (2-3) and (2-4) into the equations of momentum, we obtain

$$\eta_{1,2} = -[2(Z-1) \pm (R^2 - 8Z + 4)^{\frac{1}{2}}]/(R + 2Z) \qquad (2\text{-}5)$$

where suffixes 1 and 2 correspond to + and - in the bracket, respectively. The physical meaning of $\eta_{1,2}$ is as follows: From $\eta_1 = \eta_2$, we obtain

$$R_0 = 2(2Z-1)^{\frac{1}{2}}. \qquad (2\text{-}6)$$

This internuclear distance is the maximum distance beyond which no electron capture is expected to occur. Thus, the collision process is considered as follows:

(1) for $R>R_0$ ($t<0$), the classically allowed region is $-1\leq\eta\leq\eta_2$; that is, the electron is bound to the hydrogen atom.

(2) for $R<R_0$, the classically allowed region is $-1\leq\eta\leq1$, that is, the electron can move around both centers.

(3) for $R>R_0$($t>0$), the classically allowed region is $\eta_1\leq\eta\leq1$ or $-1\leq\eta\leq\eta_2$, depending on whether or not the electron capture occurs.

Let us define the surface F by the following equation:

$$\eta = \eta_m = -2(Z-1)/(R+2Z),\ 1\leq\xi\leq\xi_1,\ 0\leq\phi\leq 2\pi \tag{2-7}$$

where η_m is the point where the potential $V(\eta)$ exhibits a maximum. When $R<R_0$, the surface F divides the whole classically allowed volume for electron motion into two parts: V_1 (which is defined by the condition $-1\leq\eta\leq\eta_m$) and V_2 (which is defined by the condition $\eta_m\leq\eta\leq 1$). When the electron is localized in volume V_1 or V_2, the electron is considered to belong to the proton or the bare ion, respectively. We can consider the event in which the electron, localized in the volume V_1, goes through the surface F into the volume V_2, as the electron capture. Assuming that, once the electron is captured by the multiply charged ion, the strong Coulomb field of this ion makes the recapture of the electron by the proton unlikely, the electron capture probability per unit time is written

$$W(R) = (2/R^2)\int_1^{\xi_1}\frac{d\xi}{(\xi^2-1)p(\xi)}\Bigg/\int_1^{\xi_1}\int_{-1}^{\eta_m}\frac{(\xi^2-\eta^2)d\xi d\eta}{(\xi^2-1)p(\xi)(1-\eta^2)p(\eta)}\,. \tag{2-8}$$

The electron capture probability per collision with a given impact parameter is found to be

$$p(b) = \begin{cases} 1 - \exp[-(2/v)\int_b^{b_0} W(R)RdR/(R^2-b^2)^{\frac{1}{2}}] & \text{for } b<R_0 \\ 0 & \text{for } b>R_0\,. \end{cases} \tag{2-9}$$

For ionic charge Z<10, this model is expected to be valid in the intermediate range of 10 - 100 keV/amu, while the applicability for larger ionic charge is extended toward lower energies(i.e., E>0.5 keV/amu for Z≈30).

The calculation of the transition probability using this model is easier than that using the close-coupling method or classical trajectory Monte Carlo method (CTMC), but it is not a spare-time work. Ryufuku et al.[2] have proposed more simplified OBM. In their OBM, the motion of the electron is considered only in one dimension. The motion of the electron is restricted to the direction along the internuclear axis between the bare ion and proton. Using this model, the cross section can be written

$$\sigma = \tfrac{1}{2}\pi R_p^2 \qquad (2\text{-}10)$$

where

$$R_p = 2(Z-1)/[(Z^2/n_p^2) - 1] \qquad (2\text{-}11)$$

and n_p is the principal quantum number of the bare ion where the electron is transferred and is written as follows:

$$n_p = [\{(2Z^{\frac{1}{2}} + 1)/(Z + 2Z^{\frac{1}{2}})\}^{\frac{1}{2}}]\, Z \qquad (2\text{-}12)$$

Here the squared bracket [x] is the Gauss symbol to denote taking a largest integer not exceeding x.

We have interpreted the OBM for one-electron system. For the cases where the target is not hydrogen atom and (or) where the projectile ion is not bare, the OBM can be applied by using the effective nuclear charge. Recently, some extensions of the above mentioned simplified OBM have been done by Barany et al[3]. and Niehaus[4].

2.2 Multichannel Landau-Zener model

According to the Landau - Zener (LZ) model[5,6], the transition probability between two adiabatic states (1 and 2) at a pseudocrossing at the internuclear distance R_c is given by

$$p = \exp(-2\pi U_{12}^2 / v_R \Delta F) \tag{2-13}$$

where

$$\Delta F = [d(U_{11} - U_{22})/dR]_{R=R_c} \tag{2-14}$$

and the radial velocity at the crossing point is

$$v_R = v_\infty [1 - U_{11}(R_c)/E - b^2/R_c^2]^{\frac{1}{2}} . \tag{2-15}$$

Here U_{12} is the relevant coupling matrix element, v_∞ and E are the collision velocity and energy, respectively, U_{11} and U_{22} are the diabatic

potential energies and b is the impact parameter. The coupling matrix element can be determined by the method discussed by Bates and Moiseiwitch[7]. Using their method, Salop and Olson[8] have presented the analytical formula for evaluating this matrix element. On the other hand, we can also employ the empirical formula obtained by Olson et al[9]. It must be noted that in deriving the Landau-Zener probability two assumptions have been made. The first assumption is that in the vicinity of the crossing the magnitude of the interaction is constant. The second is that the diabatic potential energies, U_{11} and U_{22}, as a function of the internuclear distance are replaced by their tangents at R_c. Thus,

$$U_{11} - U_{22} = C_0(R - R_c) \qquad C_0 > 0 \ . \tag{2-16}$$

For the case where there are only two states and a single crossing, the total transition probability after two transversals of the crossing region during the collision is approximated by summing over two possible ways of making the transitions and is given by

$$P_{12} = 2p(1-p). \tag{2-17}$$

In deriving this equation, the phases, which are developed along the trajectories and are introduced at the crossing point,[10] have been neglected. The total cross section is

$$\sigma_{LZ} = 2\pi \int P_{12} b db = 4\pi R_c^2 [1 - U_{11}(R_c)/E] G(g) \tag{2-18}$$

where G(g) is the following universal function:

$$G(g) = \int_1^{\infty} \exp(-gx)[1 - \exp(-gx)]dx/x^3. \qquad (2\text{-}19)$$

Since this universal function has a maximum value of 0.113 at g = 0.42, the maximum value of the cross section is $0.452\pi R_c^2$.

This method has been extended to a multichannel system and applied to the electron capture by bare ions from hydrogen atom by Salop and Olson[8]. They assumed that the crossings occur only between the initial state 0 and electron capture states j (j=1,2,...,N) and that the corresponding crossing regions are well separated from each other. By summing over the possible paths necessary to make the transition from state 0 to state j, the equation of the total probability for the electron capture to the state j is given by

$$\begin{aligned} P_j = p_1 p_2 \cdots p_j(1-p_j)[1+(p_{j+1}p_{j+2}\cdots p_N)^2 \\ + (p_{j+1}p_{j+2}\cdots p_{N-1})^2(1-p_N)^2 \\ + (p_{j+1}\cdots p_{N-2})^2(1-p_{N-1})^2 + \cdots \\ + p_{j+1}^2(1-p_{j+2})^2 + (1-p_{j+1})^2] \end{aligned} \qquad (2\text{-}20)$$

where $1 \le j \le N$ and the transition probabilities p_j are evaluated using equation (2-13).

The diabatic crossing distance R_c is given by

$$R_c \simeq 2(Z-1)(Z^2/n^2 - 1)^{-1}, \quad n \le Z \qquad (2\text{-}21)$$

where n is the principal quantum number of the channel concerned. The LZ probability (2-13) is applicable only when both the initial and final states have the same symmetry. Since the initial channel has Σ-symmetry, the LZ probability is applicable only for the Σ-Σ transition. It is well known that for one electron system in the two center Coulombic field, among the Σ states having the parabolic quantum numbers [n, n_1,n_2, m] ($n=n_1+n_2+m+1$), only the Σ-state with $n_1=m=0$ interacts with the initial channel by a strong radial coupling.

The multichannel LZ model presented here neglects the electron capture caused by the rotation of the internuclear axis. This leads to an underestimation of the cross section in low energy region by a factor of about two. This rotational mixing was taken into account in the LZ model by Demkov et al[11]. Janev et al.[12] have proposed the equation of the multichannel LZ model including rotational mixing for the total transition probability.

It should be noted that the validity of the LZ model is restricted to the adiabtic energy region. Furthermore, the multichannel LZ model, even with the rotation of the internuclear axis included, significantly overestimates the partial cross sections for state n with $n<n_m$, while it drastically underestimates them for $n>n_m$. Here n_m is the principal quantum number where the cross section becomes maximum. Since the ionic states of n>Z do not cross the initial state, the partial cross section for such states can not be evaluated by the multichannel LZ model.

One of the physical background that LZ formula can be applied successfully is the localization of the interaction region between diabatic levels. Usual LZ model was restricted only to transfer or excitation efffect due to the radial component of the relative motion. Transitions due

to rotational motion of the internuclear axis during atomic collision are considered in the two-state approximation by Russek[13]. Rotational coupling matrix element spreads over a wider range of the internuclear distance, because differential operator with respect to the angle of internuclear axis can be relpaced by the operator of the angular part of electron coordinate in the body-frame. In this case, LZ type formulas are not applicable to these transitions as they stand. This is due to the peculiar analytical properties which are different from those of the radial transition. We can write the total Hamiltonian of a diatomic system as follows:

$$H = -\frac{1}{2\mu R^2}\frac{\partial}{\partial R}\left(R^2\frac{\partial}{\partial R}\right) + H_{rot} + H_{el} + H_{cor} \qquad (2\text{-}22)$$

where

$$H_{rot} = -\frac{1}{2\mu R^2}\left[\frac{1}{\sin\Theta}\frac{\partial}{\partial\Theta}\left(\sin\Theta\frac{\partial}{\partial\Theta}\right) + \frac{1}{\sin^2\Theta}\frac{\partial^2}{\partial^2\Phi}\right], \qquad (2\text{-}22')$$

μ is the reduced mass of the collision system, H_{rot} is the rotational Hamiltonian of the diatomic molecule, H_{el} is the electronic Hamiltonian, and H_{cor} denotes the Coriolis interaction given by

$$H_{cor} = \frac{1}{2\mu R^2}L^2 - \frac{1}{2\mu R^2}(L_+U_+ + L_-U_-), \qquad (2\text{-}23)$$

with

$$L_\pm = L_\xi \pm iL_\eta \qquad (2\text{-}24)$$

and

$$U_\pm = \mp\frac{\partial}{\partial\Theta} + \frac{i}{\sin\Theta}\frac{\partial}{\partial\Phi} + L_\zeta\cot\Theta. \qquad (2\text{-}25)$$

The angles Θ and Φ are the ordinary angle variables to define the molecular axial orientation, L is the electronic angular momentum vector and L_ξ, L_η and L_ζ are the components of L in the molecular fixed-coordinate system with the ζ-axis along the internuclear axis and ξ and η are perpendicular to ζ. In the radial coupling (usual LZ model) cases, the eigen states of H_{el} are taken as the basis functions and H_{cor} does not appear becasue of different symmetry. In the rotational coupling cases if we take the eigen states of $H_{el} + H_{rot} + H_{cor}$ as the basis function (dynamical basis), the interaction between the eigen states can be taken by

$$-\frac{1}{2\mu R^2}\frac{\partial}{\partial R}\left(R^2\frac{\partial}{\partial R}\right) , \qquad (2\text{-}26)$$

just the same as in the case of radial coupling. By taking dynamical basis function, the interaction can be confined into small region of R and LZ formulas can be taken in a way similar to the usual LZ method. This dynamical basis theory for rotational coupling has been formulated and extended by Nakamura and his coworkers[14,15], and was applied to the case of $Li^+ + Na$ and $Na^+ + Li$ collisions[16]. It will be possible to extend this method for the change transfer probability involving highly charged ions.

References

1. T.P. Grozdanov, J. Phys. B13, 3835 (1980).
2. H. Ryufuku, K. Sasaki and T. Watanabe, JAERI memo 8387 (1979); Phys. Rev. A 21, 745 (1980).
3. A. Barany, G. Astner, H. Cederquist, H. Danared, S. Huldt, P. Hvelplund, A. Johnson, H. Knudsen, L. Liljeby and K. G. Rensfelt, Nucl. Instr. Meth. B9, 397 (1985).
4. A. Niehaus, J. Phys, B19, 2925 (1986).
5. L. Landau, Phys. Z. Sowjetunion 2, 46 (1932).
6. C. Zener, Proc. R. Soc. London A137, 696 (1932).
7. D.R. Bates and B.L. Moiseiwitsh, Proc. Phys. Soc. A67, 805 (1954).
8. A. Salop and R.E. Olson, Phys. Rev. A13, 1312 (1976).
9. R. E. Olson, F. T. Smith and E. Bauer, Appl. Opt. 10, 1848 (1971).
10. E. C. G. Stueckelberg, Helv. Phys. Acta. 5, 369 (1932).
11. Yu. N. Demkov, V. N. Ostrovskii and E.A. Solv'ev, Zh. Eksp. Teor. Fiz. 66, 125 (1974) (Sov. Phys. - JETP 39, 57 (1974)).
12. R. K: Janev, D.S. Belic, and B.H. Bransden, Phys. Rev. A28, 1293 (1983).
13. A. Russek, Phys. Rev. A4, 1918 (1971).
14. H. Nakamura and M. Namiki, J. Phys. Soc. Jpn. 49, L843 (1980); Phys. Rev. A24, 2956 (1981); A28, 486 (1983).
15. H. Nakamura, Phys. Rev. A26, 3125 (1982); A28, 486 (1983).
16. R. Suzuki, H. Nakamura and E. Ishiguro, Phys. Rev. A29, 3060 (1984).

3. Classical trajectory Monte Carlo method (CTMC)

The classical equations of motion for a three-body system interacting with one another can be solved accurately by means of a modern high-speed computer in contrast to the corresponding Schrodinger equation which is difficult to solve without any approximate procedure[1-3]. Though the relation between the quantal and the classical results has not been clarified in a rigorous manner, it has been proved empirically that the classical mechanics gives results close to the quantal calculations in such cases as charge transfer processes.

One may suppose that the long-range nature of the Coulomb interaction is one of the reasons which make the classical mechanics applicable to those processes. In fact, the Rutherford scattering cross section is correctly given by the classical mechanics. However, Rutherford scattering is a two-body problem and we can not extend this finding directly to the three-body scattering problem because the latter involves partly bound states of two-body subsystems, in which pure quantal effects such as discretization of energy levels are important. Bransden and Janev[4] implies that the O(4) dynamical symmetry inherent in the one-electron atomic system and the separability of the coordinates in the two-center Coulomb system are the reasons of the success in the capture processes between a hydrogen atom and a multicharged naked ion. Their suggestion is impressive but we can not accept it easily because it is difficult to expect that the classical mechanics abruptly breaks down as we go further to the problems of two- or multi-electron systems.

The classical Hamiltonian for a three-body system is given by

$$H = \tfrac{1}{2}\,[1/m_A + 1/m_C]\; p^2_{A\text{-}C} + \tfrac{1}{2}[1/m_B + 1/(m_A + m_C)]\,p^2_{AC\text{-}B} + V_{A\text{-}B} + V_{B\text{-}C} + V_{C\text{-}A} \qquad (3\text{-}1)$$

where m_A, m_B and m_C are the masses of the particles A, B, and C, respectively, and the part of the center-of-mass motion of the whole system has been excluded. $V_{A\text{-}B}$, $V_{B\text{-}C}$ and $V_{C\text{-}A}$ are the interactions between the pairs A-B, B-C and C-A, and $P_{A\text{-}C}$ and $P_{AC\text{-}B}$ are the momenta between A and C and between the pair (AC) and B, respectively. The kinetic energy part can be expressed in three different forms according to the choice of the Jacobi coordinates. The classical motion of the particles is described by Hamilton's canonical equations of motion:

$$\frac{dq_i}{dt} = \frac{\partial H}{\partial p_i}\,, \quad \frac{dp_i}{dt} = -\frac{\partial H}{\partial q_i} \qquad (i = 1 - 6) \qquad (3\text{-}2)$$

where q_i and p_i are the components of the coordinates and momenta of the relevant relative motions. (q_1, q_2, q_3) represent the coordinates of the relative motion between A and C and (q_4, q_5, q_6) represent those between (AC) and B.

The twelve coupled equations are solved under the randomly selected initial conditions which simulate statistically the quantum-mechanical distribution of probability of the particles. The initial internal state of the target atom is usually represented by the microcanonical ensemble[5] in which the square of the eccentricity of the elliptical orbit is uniformly distributed. In this distribution the substates belonging to the same binding energy but to different angular momentum quantum numbers (ℓ, m) are uniformly populated in accordance with the quantum-mechanical description, and the distribution of the momentum p summed over the substates coincides

with the quantal one which is obtained by the sum of the momentum-space wave function:

$$\rho(p) = 8\, p_n^5 \,/\, [\pi^2(p^2 + p_n^2)^4] \qquad (3\text{-}3)$$

where p_n is the representative momentum related to the eigenenergy E_n as $p_n = \sqrt{-2E_n}$. The initial quantum state of the projectile motion is distributed uniformly over the square of the impact parameter. This uniformity corresponds to the plane-wave description of the incident wave.

The probability of the relevant reaction is calculated by counting the number of events classified by the classical energy relation after the collision has finished. For example, if the energy between the particles B and C

$$E_{BC} = \tfrac{1}{2}[1/m_B + 1/m_C]p_{BC}^2 + V_{B\text{-}C} \qquad (3\text{-}4)$$

becomes negative, the particle C is identified as being in a bound state of particle B, that is, the particle C (electron) is transferred to the projectile B. The cross section for a final channel f is given by

$$\sigma_f = (N_f/N)b_{max}^2\pi \,, \qquad (3\text{-}5)$$

where N is the total number of trajectories and N_f is the number of the trajectories for which the electron remains in the state f after the collision. b_{max} is the maximum impact parameter beyond which no event of the channel f is expected to occur.

The identification of the atomic internal quantum numbers (n,ℓ) is not so easy because the binding energy and the orbital angular momentum can take non-integral values in the classical mechanics. The "quantization" of them is made by regarding the values locating in a certain width centered at a discrete quantum value as the corresponding one. In the choice of the boundaries of each width there remains some arbitrariness and ambiguity.

References

1. M. Karphus, R. N. Porter and R. D. Sharma, J. Chem. Phys. 43, 3249 (1965).
2. R. Abrines and I. C. Percival, Proc. Phys. Soc. 88, 861 (1966).
3. R. Abrines and I. C. Percival, Proc. Phys. Soc. 88, 873 (1966).
4. B.H. Bransden and R.K. Janev, Adv. At. Mol. Phys. 19, 1 (1983).
5. I.C. Percival and D. Richards, Adv. At. Mol. Phys. 11, 1 (1975).
6. A. Salop, J. Phys. B 12, 919 (1979).

4. Impact parameter approach

Since the masses of the target atom and the incident ion are large, compared with the electron mass, the impact-parameter approach is applicable to charge transfer processes involving highly charged ions except for those at energies lower than 100 eV/amu. In this approach the relative motion of the colliding pair is treated classically, meanwhile the internal (electronic) motion is treated quantum mechanically. As a result the

Hamiltonian includes the coordinates of the relative motion as a parameter which determines the interaction potential affecting the electron:

$$H = -\tfrac{1}{2}\nabla_r^2 - Z_A/r_A - Z_B/r_B - Z_A Z_B/R \qquad (4\text{-}1)$$

where $\mathbf{r}_A$ and $\mathbf{r}_B$ are the position vectors of the electron with respect to the nuclei A and B, respectively. R is the position vector of B with respect to A and is determined beforehand as a function of the time t. In addition the heavy particles can be assumed to move along a straight-line trajectory with a constant velocity v if the collision energy is higher than several hundred electron volts per atomic mass unit:

$$R(t) = b + vt \qquad (4\text{-}2)$$

where b is the impact parameter vector.

The Schrödinger equation which determines the electronic motion is given by

$$(H - i\frac{\partial}{\partial t})\Psi(r,t) = 0 \qquad (4\text{-}3)$$

where r is the position vector of the electron with respect to the coordinate origin. The wave function $\Psi(r,t)$ is expanded as the sum of basis functions ψ_n:

$$\Psi(r,t) = \sum_{n=1}^{N} a_n(t)\psi_n(r,t). \qquad (4\text{-}4)$$

Substitution of eg. (4-4) into (4-3) yields the coupled differential equations for coefficients a_n as;

$$i\underline{s}\dot{a} = \underline{h}a \ , \tag{4-5}$$

where a is the state vector whose components are the expansion coefficients $\{a_n\}$ and the overlap matrix $\underline{s}$ and the interaction matrix $\underline{h}$ are defined as

$$s_{ij} = \int \psi_i^*(\mathbf{r},t)\psi_j(\mathbf{r},t)d\mathbf{r}, \tag{4-6}$$

$$h_{ij} = \int \psi_i^*(\mathbf{r},t)(H - i\frac{\partial}{\partial t})\psi_j(\mathbf{r},t)d\mathbf{r}. \tag{4-7}$$

Since the internuclear distance R is the function of t and independent of r, it can be eliminated from the Hamiltonian by the following transformation:

$$\Psi(\mathbf{r},t) = \Psi_0(\mathbf{r},t)\ \exp(-i\int dt' Z_A Z_B/R) \ . \tag{4-8}$$

From the above expression we realize that the internuclear interaction affects only the phase of the wave function; that is, the transition probability does not depend on the interaction if the straight-line trajectory is employed. Keeping this knowledge in mind we often drop the internuclear interaction. However it should be noted that we must take this phase factor into consideration explicitly in calculation of the differential cross sections.

4.1. Atomic orbital expansion

When the relative velocity between the nuclei is larger than the average orbital velocity of the transferred electron, we can expect that the nature of the electronic wave functions does not deviate significantly from that of the atomic states. Thus the choice of atomic orbitals $\{\phi_n\}$ for the basis functions ψ_n in equation (4-4) is convenient in intermediate or high energy region:

$$\psi_n = \phi_n(r_A) \exp(-i\epsilon_n t)F \ , \tag{4-9}$$

where ϵ_n is the energy of the state ϕ_n and F is the atomic electron translation factor (ETF) defined as

$$F = \exp(iv_{A,B} \cdot r + \frac{i}{2}v_{A,B}^2 t) \ . \tag{4-10}$$

v_A and v_B are the velocity vectors of the nuclei A and B with respect to the coordinate origin. If the origin is located on the internuclear axis and divides it as p:q (p+q=1) then v_A=-pv and v_B=qv. The atomic orbitals centered at different nuclei are generally nonorthogonal to each other so that we must calculate the overlap matrix at each time step. Multiplying the inverse matrix of $\underline{s}$ we obtain

$$\dot{a} = -i\underline{s}^{-1}\underline{h}a \ . \tag{4-11}$$

The matrix $\underline{h}$ is not hermitian but it satisfies

$$i\underline{\dot{s}} = \underline{h}^{\dagger} - \underline{h} \qquad (4\text{-}12)$$

where $\underline{h}^{\dagger}$ denotes the hermite conjugate of the matrix $\underline{h}$. As a consequence $\underline{s}^{-1}\underline{h}$ is not hermitian and the conservation of probability (unitarity) is not represented by $|a|^2 = 1$ but as

$$a^{\dagger}\underline{s}a = 1 \quad \text{at any time } t. \qquad (4\text{-}13)$$

As $\underline{s}$ becomes unit matrix at the infinity $t=\infty$, a retrieves its unitarity there.

The calculated results often agree with experimental data down to energies lower than expected. One reason of the agreement at low energies arises from the fact that charge transfer cross sections are mainly determined at relatively large impact-parameters, where the atomic nature of the wave function is reserved.

In order to take into consideration the ionization channel, which may play an important role as the intermediate states, the pseudostates are occasionally incorporated into the basis functions. The pseudostates also play a part of molecular states in the united-atom limit. Winter and Lin[1] made a triple-center expansion, in which the third center is located at the center of charge. The increase of the basis functions and the expansion centers certainly improves the description of the wave function but, as a matter of fact, the required labor and computational time increases in return.

4.2. The unitarized distorted wave approximation

Ryufuku and Watanabe[2] presented an approximate expansion procedure based on the distorted-wave formalism. The matrix $\underline{H}=\underline{s}^{-1}\underline{h}$ is divided into two parts:

$$\underline{H} = \underline{H}^{0} + \underline{H}^{int}, \tag{4-14}$$

where $\underline{H}^{0}$ is a matrix composed only of the diagonal part of $\underline{H}$. The S matrix defined as

$$a(t=\infty) = \underline{S}\, a(t=-\infty) \tag{4-15}$$

can be written as

$$\underline{S} = \exp(-i \int_{-\infty}^{\infty} \underline{H}^{0}\, dt)\, \underline{S}^{int}, \tag{4-16}$$

where

$$\underline{S}^{int} = T \exp(-i \int_{-\infty}^{\infty} \hat{\underline{H}}^{int}(t)\, dt), \tag{4-17}$$

with

$$\hat{\underline{H}}^{int} = \exp(i \int_{-\infty}^{t} \underline{H}^{0}\, dt)\, \underline{H}^{int} \exp(-i \int_{-\infty}^{t} \underline{H}^{0} dt) \tag{4-18}$$

and T is the chronological operator. The above expressions are still exact. They introduced the following approximations keeping the unitarity of the S matrix:

(i) drop the operator T.

(ii) include only the initial state for the atom A and ignore all the matrix elements which are not related to the initial state directly.

(iii) expand s^{-1} and retain terms up to the first order with respect to the overlap matrix element s_{ij}. The transition amplitude for the electron capture from the initial state $|0\rangle$ to a final state $|n\rangle$ is given by

$$\langle n|\underline{S}|0\rangle = it_{n0}\, p^{-1/2} \sin p^{1/2}, \tag{4-19}$$

where

$$p = \sum_n |t_{n0}|^2 \tag{4-20}$$

and t_{n0} is the transition amplitude of the distorted-wave Born approximation;

$$t_{n0} = \int_{-\infty}^{\infty} dt\, (h_{n0} - s_{n0}h_{00}) \exp\left[i\int_{-\infty}^{t} (\varepsilon_n - \varepsilon_0 + h_{nn} - h_{00})dt'\right] . \tag{4-21}$$

Though it is rather difficult to assess the reliability of the approximations employed in the UDWA quantitaively and its limitation of the

applicability rigorously, the cross sections predicted by the UDWA have been proved to be in good agreement with experimental data over a surprisingly wide energy region. As for the second approximation, Suzuki et al.[3] examined the contribution of the couplings among the final states and developed a revised version named the exponential distorted wave approximation (EDWA). They found that the difference between the UDWA and the EDWA cross sections is small down to a few keV/amu and the couplings among the final states are not important there. Generally speaking, the third approximation is valid when the distant collisions dominate the scattering processes. This is really the case for the electron capture from a hydrogen atom by multicharged naked ions.

One of the features of the UDWA is that it can incorporate the contribution of an exceedingly large number of the states. As the nuclear charge of the projectile increases, the number of the final excited states which contribute to the capture process increases rapidly. Another is the consideration of the distortion effect of the atomic orbitals due to the Coulomb interaction. This distortion is an important factor that determines the principal quantum number $\bar{n}$ of the states to which the electron is transferred most effectively. The prediction for the averaged principal quantum number $\bar{n} = z^{0.774}$ agrees well with other calculations and experimental findings.

4.3. Perturbative approach

We can expect that the perturbation theory generally works better as the collision energy becomes higher. However, as for the electron capture processes, we have to pay special attention to its applicability. The

ordinary first-order Born approximation called the Brinkmann-Kramers (BK) approximation[4], in which only the interaction between the electron and the projectile (or the target) is incorporated, gives the considerably overestimated cross sections. One of the reasons of this overestimation is due to the lack of orthogonality between the atomic orbitals of the initial and the final states. Bates[5] modified the first-order treatment by taking into account the non-orthogonality explicitly and the agreement with experimental data has been improved to great extent. On the other hand, it was shown that the addition of the internuclear interaction to the BK formula, which is called the Jackson and Schiff (JS) approximation[6,7] or the full Born approximation, reduces the cross sections and makes them closer to experimental values in proton-hydrogen capture processes. However, this agreement is proved to be fortuitous because the JS approximation gives cross sections which are greater than the experimental data by several orders of magnitude in the case of highly asymmetric system such as the capture to the K-shell of argon ion from hydrogen atom.

The BK and JS approximations possess both the pure-quantal and impact-parameter versions, which give identical results at high energy region.

Dewangan[8] has applied the eikonal approximation to proton-hydrogen system and has shown that the eikonal cross section can be represented as a product of the BK and a factor which is a slowly varying function of the collision velocity. The transition amplitude in the prior form is represented as

$$a_f = -i\int_{-\infty}^{\infty} dt \langle \psi_f(r_B) | -Z_B/r_B | \phi_i(r_A) \exp(-i\Delta E t) , \qquad (4\text{-}22)$$

where ΔE is the energy difference between the initial and the final atomic states and $\phi_i(r_A)$ is the initial atomic wave function with an appropriate ETF and the eikonal phase factor;

$$\Psi_f(r_B) = \phi_f(r_B) \exp(-i\int_t^\infty z_A/r_A \, dt'). \qquad (4\text{-}23)$$

Chan and Eichler[9] applied this approximation to electron capture processes from hydrogen atom by multicharged naked ion.

It is widely recognized that the leading term in the high energy limit is the double scattering process which is adequately described by the second Born approximation[10]. Those perturbative treatments mentioned above do not include it. On the contrary, the impulse approximation[11] and the continuum distorted-wave (CDW) approximation[12] include this contribution and the high energy behavior of their cross sections coincides with that predicted by the second Born approximation.

Recently Dewangan and Eichler[13] have pointed out that the disagreement of OBK with experimental data in high impact velocity is due to the long-range nature or the Coulomb potential. The operators in the transition amplitude should be taken to match the asympotic condition of the incident and scattered wavefunctions. In order that the asymptotic forms of wavefunctions are well defined, the operators in the first order of Born amplitute are desired to be of sufficiently short range, such as

$$a_f = i\int_{-\infty}^{\infty} \langle \Phi_f \exp[i\nu_T \ln(R + vt)] | Z_T/r_T - Z_p/R | \Phi_i \exp[i\nu_p \ln(R - vt) \rangle dt \qquad (4\text{-}24)$$

where R, r_T, Z_T and Z_p are the internuclear distance, the distance between the electron and the target nucleus, target nuclear charge and projectile nuclear charge, respectively. Φ_i and Φ_f include the translational factors and $\nu_T = Z_T(Z_p - 1)/v$, and $\nu_p = Z_p(Z_T - 1)/v$. It turns out that the first-order amplitude which is consistent with the long-range nature of the Coulomb interaction yields reasonable agreement with data even without any further correction.

4.4 Molecular orbital expansion

When the collision velocity is smaller than the orbital velocity of the active electron, we can use, as the basis functions, the adiabatic molecular wavefunctions χ_n:

$$\Psi_n = \chi_n(\mathbf{r},R) \exp(-iE_n t) F. \tag{4-25}$$

Here E_n is the adiabatic energy of the state χ_n obtained by

$$H_{el} \chi_n(\mathbf{r},R) = E_n(R) \chi_n(\mathbf{r},R) \tag{4-26}$$

where H_{el} is the electronic Hamiltonian and F is the electron translation factor (ETF). Since the molecular basis is employed for the case of small collision velocity, the calculation of the cross section including ETF was scarcely performed until about ten years ago. The neglect of ETF makes the

coupled equation considerably simple. As a result, the expansion coefficient corresponding to the i-th channel is written as follows:

$$\dot{a}_i(t) = -\sum_j (v_R V^R_{ij} + \dot{\theta} V^{\theta}_{ij}) \exp[-i\int_{-\infty}^{t} (E_j - E_i)dt']a_j(t) \qquad (4\text{-}27)$$

where v_R is the radial velocity, $\dot{\theta} = v_\infty b/R^2$ is the angular velocity of the internuclear axis, v_∞ is the velocity at $R=\infty$ and b is the impact parameter. The radial coupling matrix element V^R_{ij} is given by

$$V^R_{ij} = \langle X_i(\mathbf{r},R) | (\partial/\partial R) | X_j(\mathbf{r},R) \rangle \qquad (4\text{-}28)$$

and the rotational coupling matrix element V^{θ}_{ij} is given by

$$V^{\theta}_{ij} = \langle X_i(\mathbf{r},R) | iL_y | X_j(\mathbf{r},R) \rangle, \qquad (4\text{-}29)$$

where L_y is the electronic angular momentum operator around the y axis. Here the z axis is assumed to be along the internuclear line and the y axis is perpendicular to the scattering plane.

This molecular orbital close coupling method has a fundamental drawback resulting from the absence of ETF. The wavefunctions do not have a proper

asymptotic behavior. Moreover, the coupling matrix elements depend on the coordinate origin and some of them tend to be constant values at large internuclear distances. During the past ten years, many attempts taking ETF into the coupled equation have been made. In 1978 Thorson and Delos[14] have solved this problem at least formally. They wrote ETF as follows:

$$F(\mathbf{r},R) = \exp[ivrf(\mathbf{r},R)] \tag{4-30}$$

where $f(\mathbf{r},R)$ is a switching function and has the following properties:

$$\lim_{R\to\infty} f(\mathbf{r},R) = \begin{cases} +1 & \text{if } (r_B/R) > 0 \\ -1 & \text{if } (r_A/R) > 0 \ . \end{cases} \tag{4-31}$$

However, apart from equation (4-31), there is no criteria for their construction at present. An optimal choice of the switching function can be performed by using the variational method[15]. The Euler-Lagrange equations for switching function have to be solved simultaneously with the coupled equations for the expansion coefficient. Besides this method, the plane-wave type ETF[16] and many kinds of parametric forms of ETF[17,18] obtained from the physical intuition have been employed in practical applications.

The switching function depends on states in general. In this case, the matrix $\underline{h}$ in equation (4-11) is not hermitian and the overlap matrix $\underline{S}$ is not

unit matrix. As a result, the coupled equation becomes complex and in order to solve the equation much labor and computational time are required. For small velocity collision, often the switching function is expanded with respect to the velocity and only the term up to the first order is retained. If furthermore the switching function can be assumed to be common to all states, the coupled equations take a form similar to equation (4-27) with modified coupling matrix elements, W^R_{ij} and W^θ_{ij}, as given by

$$W^R_{ij} = V^R_{ij} + \tfrac{1}{2}\langle X_i(\mathbf{r},R)\,|f(\mathbf{r},R)z|\,X_j(\mathbf{r},R)\rangle(E_j - E_i),$$
$$W^\theta_{ij} = V^\theta_{ij} + \tfrac{1}{2}R\langle X_i(\mathbf{r},R)\,|f(\mathbf{r},R)x|\,X_j(\mathbf{r},R)\rangle(E_j - E_i) \qquad (4\text{-}32)$$

where x and z are the perpendicular and parallel components of r with respect to the molecular axis, respectively.

For relative velocities below $v \tilde{<} 0.1$, the cross section may not be influenced by ETF so much in some cases, but for v>0.3 their influence becomes significant. With increasing the basis size, the results become less sensitive to the choice of ETF.

References

1. T.G. Winter and C.D. Lin, Phys. Rev. A29, 567 (1984).
2. H. Ryufuku and T. Watanabe, Phys. Rev. A19, 1538 (1979).
3. H. Suzuki, N. Toshima, T. Watanabe and H. Ryufuku, Phys. Rev. A39, 539 (1984).

4. H.C. Brinkmann and H.A. Kramer, Proc. Acad. Aci. Amsterdam 33, 973 (1930).
5. D.R. Bates, Proc. Roy. Soc. A247, 294 (1953).
6. J.D. Jackson and H. Schiff, Phys. Rev. 89, 359 (1953).
7. D.R. Bates and A. Dalgarno, Proc. Phys. Soc. A65, 915 (1952).
8. D.P. Dewangan, J. Phys. B8, L119 (1975), ibid. B10, 1083 (1977).
9. F.T. Chan and J. Eichler, Phys. Rev. Lett. 42, 58 (1979).
10. R. Shakeshaft and L. Spruch, Rev. Mod. Phys. 51, 369 (1979).
11. J.S. Briggs, J. Phys, B10, 3075 (1977).
12. I.M. Cheshire, Proc. Phys. Soc. 84, 89 (1964).
13. D.P. Dewangan and J. Eichler, J. Phys. B18, L65 (1985); ibid. B19, 2939 (1986).
14. W.R. Thorson and J.B. Delos, Phys. Rev. A18, 117 135(1978).
15. M.E. Riley and T.A. Green, Phys. Rev. A4, 619 (1971).
16. D.R. Bates and R. McCarroll, Proc. Roy. Soc. A245, 175 (1958).
17. S.B. Schneiderman and A. Russek, Phys. Rev. 181, 311 (1969).
18. J. Vaaben and K. Taulbjerg, J. Phys. B14, 1815 (1981).

5. Experimental techniques

In order to experimentally determine the (n,ℓ) distribution in electron capture processes, the following three spectroscpic methods are commonly used: 1) translational energy (or energy-gain/loss) spectroscopy[1], 2) photon spectroscopy[2] and 3) electron spectroscopy[3].

In the translational energy spectroscopy technique, the energy-gain or -loss of projectile ions which have captured electron is measured by electrostatic

or magnetic energy analyzer. The advantages of this method are high detection efficiencies and straightforward interpretation of experimental data. In fact, the measurements can be made with the projectile intensities as low as 100 cps. On the other hand, the inherent low energy resolution (at best 0.2-0.5 eV) does not allow us to discriminate the contribution from (n,ℓ) states with the same n, except for some limited cases. Thus, usually this method can provide information only on the n-distributions.

In the photon spectroscopy technique, the characteristic photons emitted from the projectile ions which have captured an electron into an excited state and decayed into lower state are measured. Since the energy resolution of photon spectroscopy is much better than that of translational energy spectroscopy, the differentiation among different (n,ℓ) states is relatively easy. However, the detection efficiencies of photons are very low and, therefore, intense ion beam sources are required. Even through the energy resolution is good, the interprelation of the observed results is not simple. Accurate wave-lengths of transitions and their probabilities (branching ratios) of electron-captured ions have to be known. A wide range of photon energies have to be measured and usually no single spectrometer can cover the whole range of photon energies concerned. The calibration of the absolute efficiencies of spectrometers is sometimes quite difficult, in particular in ultra-violet or very-ultra-violet region. Furthermore, data of transition probabilities of highly ionized ion are incomplete[4] and have to be extrapolated from the known data. The cascade contribution and polarization effect to the observed photon data should be corrected properly. Thus the overall uncertainties of the data on photon emissions (emission cross section) are large (20 - 50% at best and usually more than that). Further, the absolute cross sections of electron capture

into (n, ℓ) states should contain more uncertainities due to uncertainties of transition probabilities.

In electron spectroscopy technique, electrons emitted from projectile ions are energy-analyzed. As one-electron capture processes dominantly result in photon emission in most cases, the cross sections for only limited cases, for example two-electron capture processes into the autoionizing states, are measured with this method.

References

1. D. Dijkkamp, A. Brazuk, A.G. Drentje, F.J. de Heer and H. Winter, J. Phys. B 17, 4327 (1984).
2. K. Okuno, H. Tawara, T. Iwai, M. Kimura, N. Kobayashi, A. Matsumoto, S. Ohtani, S. Takagi and S. Tsurubuchi, Phys. Rev. A 28, 127 (1983).
3. A. Bordenave-Montesquieu, P. Benoit-Cattin, A. Gleizes, A.I. Marrakchi, S. Dousson and D. Hitz, Nucl. Instr. Meth. in Phys. Res. B 9, 389 (1985).
4. A. Lindgard and S.E. Nielsen, At.Data and Nucl. Data Tables 19, 533(1977).

6. Comparison between theory and experiment

Because of technical difficulties, only a few experiments on (n, ℓ) distribution of electron capture in multiply charged ions collided with neutral atoms have been reported. In this section, two examples are shown which have been studied fairly systematically in both theory and experiment:

$$C^{3+}\ (1s^2 2s)^2S + H(1s) \rightarrow C^{2+}\ (1s^2\ 2\ell n\ell'\ ) + H^+ \qquad (6\text{-}1)$$

and

$$C^{6+} + H(1s) \rightarrow C^{5+}\ (n,\ \ell) + H^+. \qquad (6\text{-}2)$$

6.1 $C^{3+}\ (1s^2 2s)^2S + H(1s) \rightarrow C^{2+}\ (1s^2\ 2\ell n\ell'\ ) + H^+$ process

As this process is important in interstellar cloud, some theoretical investigations, in particular those at very low energies, have been made.[1-4] Blint et al.[1] calculated the cross sections for electron capture into $(1s^2 2s3s)^3S$ and ^1S at around 1 eV. Their calculation of the energy diagram shows that the avoided crossing of the electron capture into ^3S state occurs at the internuclear distance R_c = 11.5 a.u., whereas that for ^1S state at R_c = 15 a.u. Thus the cross sections for ^1S state are small and only 1-2 % of those for ^3S state. By further extending their calculation to fully quantal calculation, Watson et al.[2] gave the cross sections for $(3s)^3S$ state over the energy range of 0.1 - 200 eV which were also compared with those by Landau-Zener calculations. Following their quantal investigation[3], Heil et al.[4] made the detailed studies on the potential energy surfaces where they showed two avoided crossings in both $^1\Sigma$ and $^3\Sigma$ states at R_c = 5.2 and 2.5 a.u. and 11.0 and 5.2.a.u., respectively, and then calculated the cross sections for electron capture into various states. Their calculation was extended by Bienstock et al.[5] over the energy range of 0.1 - 60 keV. All these calculations indicate the dominance of the electron capture into $(1s^2 2s3s)^3S$ state in this process.

On the other hand, this process has been studied experimentally using different techniques, namely ion-energy spectroscopy (IES) and photon spectroscopy (PS). MuCullough et al.[6] succeeded in determining the cross sections for some states by IES. However, because of the limited energy resolution of their system (∿3 eV), some states can not be separated but mixed as follows:

their $(3s)^3S$: $(3s)^1S$ included

$(3p)^3P^0$: $(3P)^1P^0 + (3d)^3D + (3d)^1D$

$(2p^2)^1S$: well separated

$(2p^2)^1D$: $(2P^2)^3P$.

Recently Ciric et al.[7] used the photon spectroscopy with much better energy resolution and succeeded in separating the cross sections for most of the important states. They noted that some states, which are neglected in theoretical calculations, could contribute to total cross sections. Thus, the detailed comparison between theory and experiment should be worth to be made.

According to the classical over-barrier model (see section 2.1), though the energy dependence can not be represented properly, the electron should be captured mostly into n=2 state (see eq.(2-12)). However, this prediction is accurately valid only for naked ions. In the present partially ionized C^{3+} ions, all the theories predict that the dominant capture occurs into $(1s^2 2s3s)^3S$ state at relatively low energies and the following processes can occur with relatively high probabilities:

$$C^{3+}(1s^2 2s)^2S + H(1s) \rightarrow C^{2+}(1s^2 2s3s)^3S + H^+ \quad (6\text{-}3)$$

$$(2s^2 2s3s)^1S \quad (6\text{-}4)$$

$$(1s^2 2s3p)^3P^0 \quad (6\text{-}5)$$

$$(1s^2 2s3p)^1P^0 \quad (6\text{-}6)$$

$$(1s^2 2s3d)^3D \quad (6\text{-}7)$$

$(1s^2 2s3d)^1D$ (6-8)

$(1s^2 2s4d)^3D$ (6-9)

$(1s^2 2p^2)^1S$ (6-10)

$(1s^2 2p^2)^1D$ (6-11)

$(1s^2 2p^2)^3P$. (6-12)

Fig.1 shows total electron capture cross sections as well as partial cross sections into $(1s^2 2s3s)^3S$ and ^1S states. Generally speaking, experimental data of total cross sections are reproduced quite well by the calculation of Bienstock et al.[5] over the whole energy range (10^{-1} - 10^2 keV) investigated[8], with the minimum value of $5 \times 10^{-16} cm^2$ at around 2 - 3 keV. On the other hand, data for $(3s)^3S$ state by McCullough et al.[6] are roughly in agreement with the calculation of Bienstock et al. but those of Ciric et al.[7] tend to level off and are apparently in disagreement with the calculation at high energies. At the moment no clear reasons can be identified for this discrepancy. However, it should be noted that total cross sections of Ciric et al. obtained by summing up all their partial cross sections are also in disagreement with the calculation and those of McCullough et al. Small cross sections for $(3s)^1S$ state observed by Ciric et al. agree qualitatively with the estimation by Blint et al.

In Fig.2 are shown data for $C^{2+}(1s^2 2s3p)^3P^0$, $(1s^2 2s3p)^1P^0$, $(1s^2 2s3d)^3D$ and $(1s^2 2s3d)^1D$ by Ciric et al. As mentioned already, data by McCullough et al. represent the sum of all these four states. Both experiments are generally in agreement with each other. It should be noted that data by PS indicate the main contribution comes from $(3d)^3D$ state at the energy higher than 10 keV, which is in contrast to the prediction of the dominance of $(3p)^3P^0$ state by Bienstock et al.

Figure 3 shows those for $(4d)^3D$ state where no theoretical estimation is available. The experimental data, which represent only 1 - 2% of total cross sections, indicate to increase with increasing the collisions energy.

Figure 4 shows those for $(1s^2 2p^2)^1S$ state which involve two electron transition, ore electron excited and the other captured. Experimental data by McCullough et al. obtained by IES are roughly in agreement with the prediction of Bienstock et al. and also agree with those of Ciric et al. at the lowest energies overlapped, the latter tending to decrease too rapidly and apparently in disagreement with calculation with increasing the energy.

A comparison is shown in Fig.5 of $(1s^2 2p^2)^1D$ and ^3P states. Bienstock et al. did not calculate those for ^3P state, apparently assuming the dominance of ^1D state. Indeed, experiment of Ciric et al. shows dominant ^1D state. The sum of ^1D and ^3P states are in agreement in both experiments.

At the energy lower than 10 eV, only theoretical calculations are available. There all theories assume the dominance of $(2s3s)^3S$ state. The cross sections are predicted to increase with decreasing the energy. This trend can be understood from the potential energy curves of this system, suggesting the avoided crossings at relatively large internuclear distances which are effective even at zero energy. It should be noted that their detailed calculation of Heil et al. gives the cross sections by a factor of two too large, compared with those by Watson et al. and Blint et al., though they tend to converge at lower energies around 10 eV. Furthermore, it should be noticed that the simple Landau-Zener calculation is in perfect agreement with the quantal calculation of Watson et al. down to 0.2 - 0.3 eV. Their quantal calculation suggests some resonances at 0.045 and 0.065 eV which remain to be confirmed experimentally (Fig.6).

The radiative electron capture process

$$C^{3+} + H \rightarrow C^{2+} + h\nu \qquad (6\text{-}13)$$

has the rate coefficients which are of the order of $10^{-14}cm^3/s$, much smaller than those for non-radiative electron capture discussed above over the temperature of $10 - 10^5 K$[9].

6.2 $C^{6+} + H(1s) \rightarrow C^{5+}(n, \ell) + H^+$ process

As this system has only one electron and there are no ambiguity and complexity arising from electron correlation, it is a good model system to test the computational methods. Furthermore electron capture by slow ($v < 1.0$ au), fully stripped ion from atomic hydrogen is very important reaction in astrophysics and fusion plasmas. Thus this system has been the subject of intensive theoretical studies. On the other hand, though there are some experiments for total cross sections, only a single experiment of Dijkkamp et al.[10] has been reported for the final state resolved cross sections.

This is because the production of the target hydrogen atoms is not so easy and the ℓ-distribution of product ions can not be determined by the efficient energy gain spectroscopy and thus measured by less efficient optical method.

We first compare typical calculations with experiments for total cross sections. Fig.7 shows the results of three elaborate impact parameter methods (the 33-state MO expansion of Green et al.[11], the 35-state AO expansion of Fritsch and Lin[12] and the AO-MO (25-state-26-state) matching method of Kimura and Lin[13]) together with the results from Landau-Zener model (Salop and Olson[14] and Janev et al.[15]), CTMC of Olson and Salop[16] and UDWA of Ryufuku[17]. The Landau-Zener model by Janev et al. includes the rotational transitions (= MLZR). Three experimental results by Phaneuf et al.[18], Panov et al.[19] and Meyer et al.[20] are also shown. There are small discrepancies among experiments. In particular, the irregularity of the energy dependency of the results by Panov et al. is conspicuous.

Ryufuku[17] and Ryufuku and Watanabe[21] have calculated the total electron capture cross sections for this system using UDWA method. Their results are in good agreement with experiment in high energy region (E>2 keV/amu). The results of MLZ by Salop and Olson[14] have the energy dependence similar to experiment but their absolute values are smaller than experiment by a factor of two or three. The results of MLZR by Janev et al.[15] are in good agreement with experiment at the energies above 0.3 keV/amu. There are no experiment and reliable close coupling calculation for the energies overlapping the results by Olson and Salop using CTMC method[16], which agree with the results of UDWA. The results of the close coupling calculation using MO[11], AO[12] and AO-MO[13] are in good agreement with each other and also with experimental results.

There is some accidental agreement among theoretical calculations for total electron capture cross sections. In order to test computational methods more critically, the final state resolved cross sections should be compared. Fig.8 shows the n-distribution of the cross sections calculated from the AO, MO and AO-MO matching methods. In this figure, the results of more feasible MO method by Bendahman et al.[22] which involves only 5 molecular states with ETF are also shown. The results for n = 4 agree with each other among the four calculations. Comparing the results of the AO, MO and AO-MO matching methods for n = 5, Kimura and Lin[13] insisted that the AO-MO results agree better with the AO results while the MO predicts much higher values. However, as shown in Fig. 8, the results of the MO method with 5 states agree pretty well with the results of the AO and AO-MO matching methods.

Fig.9 shows the calculated relative population of specific ℓ -substates within the n = 4 and 5 manifolds at incident energies E = 1.0 and 0.64 keV/amu. Salin[23] used the impact parameter method which did not consider ETF and used 11 molecular states with the coordinate origin fixd on the projectile. In his calculation, after solving the coupled equations, the coupling by Stark effect

between the states in the selected n-manifold has been considered. Fig.9(a) indicates that the results of AO are in good agreement with the results of AO-MO. Furthermore, it suprises us that the results by Salin are also in good agreement with the above two results. Fig.9(b) shows the discrepancy between the results of AO and MO at higher ℓ values.

Dijkkamp et al.[10] have observed VUV emissions for n=3 ← n=4, n=2 ← n=4 and n=2 ← n=3 transitions at 52.0, 13.5, and 18.2 nm, respectively. In order to compare the theory with these data, we constructed the emission cross sections from the calculated partial cross sections, taking into account the appropriate hydrogenic branching ratios[24] and all the cascade contributions from higher levels. Fig.10(a) compares the experiment by Dijkkamp et al. with the close coupling results of MO[11] and AO[12]. Three data are in good agreement with each other. Fig.10(b) compares the experiment by Dijkkamp et al. with the results of AO-MO matching method and of Salin. As a matter of convenience, the results of AO are also included in this figure. In contrast to very good agreement between AO and AO-MO matching methods in Figs. 7, 8 and 9, the results of AO-MO do not agree so well with the results of AO and of experiment in this figure. Furthermore, though the results by Salin are in agreement with those of AO and AO-MO as shown in Fig.9(a), those for emission cross sections do not agree so well with the latters in Fig.10(b). The other computational methods appeared in Fig. 7 are not suitable for estimating the (n, ℓ) distributions, so we did not cite these results in Fig. 8, 9 and 10 intentionally.

References

1. R.J. Blint, W.D. Watson and R.B. Christensen, Astrophys. J. 205, 634 (1976).
2. W.D. Watson and R.B. Christensen, Astrophys. J. 231 627 (1979).
3. S.E. Butler, T.G. Heil and A. Dalgarno, Astrophys. J. 241, 442 (1980).
4. T.G. Heil, S. Butler and A. Dalgarno, Phys. A 23, 1100 (1981).

5. S. Bienstock, T.G. Heil, C. Bottcher and A. Dalgarno, Phy. Rev. A 25, 2850 (1982).

6. R.W. McCullough, F.G. Wilkie and H.B. Gilbody, J. Phys. B 17, 1373 (1984).

7. D. Ciric, A. Brazuk, D. Dijkkamp, F.J.de Heer and H. Winter, J. Phys. B 18, 3629 (1985).

8. H. Tawara, T. Kato and Y. Nakai, At. Data and Nucl. Data Tables, 32, 235 (1985).

9. S.E. Butler, S.L. Guberman and A. Dalgarno, Phys. Rev. A 16, 500 (1977).

10. D. Dijkkamp, D. Ciric and F.J.de Heer, Phys. Rev. Letters 54, 1004(1985)

11. T.A. Green, E.J. Shipsey and J.C. Browne, Phys. Rev. A25, 1364(1982)

12. W. Fritsch and C.D. Lin, Phys. Rev. A29, 3039(1984)

13. M.Kimura and C.D. Lin, Phys. Rev. A32, 1357(1985)

14. A. Salop and R.E. Olson, Phys. Rev. A13, 1312(1976)

15. R.K. Janev, D.S. Belic and B.H. Bransden, Phys. Rev. A28, 1293(1983)

16. R.E. Olson and A. Salop, Phys. Rev. A16, 531(1977)

17. H. Ryufuku, Phys. Rev. A25, 720(1982)

18. R.A. Phaneuf, I. Alvarez, F.W. Meyer and D.H. Crandall, Phys. Rev. A26, 1892(1982)

19. M.P.N. Panov, A.A. Basalaev and K.O. Lozhkin, Phys. Scr. T3,124(1983)

20. F. Meyer, A.M. Howald, C.C. Havener and R.A. Phaneuf, Phys. Rev. A32, 3310(1985)

21. H. Ryufuku and T. Watanabe, Phys. Rev. A19, 1538(1979)

22. M. Bendahman, S. Bliman, S. Dousson, D. Hitz, R. Gayet, J. Hanssen, C. Harel and A. Salin, J. Phys. (Paris) 46, 561(1985)

23. A. Salin, J. Phys.(Paris) 45, 671(1984)

24. W.L. Wiese, M.W. Smith and B.M. Glennon, Atomic Transition Probabilities, U.S. National Bureau of Standards, National Standards Reference Data Series - 4 (U.S. GPO, Washington, D.C., 1966), Vol. 1.

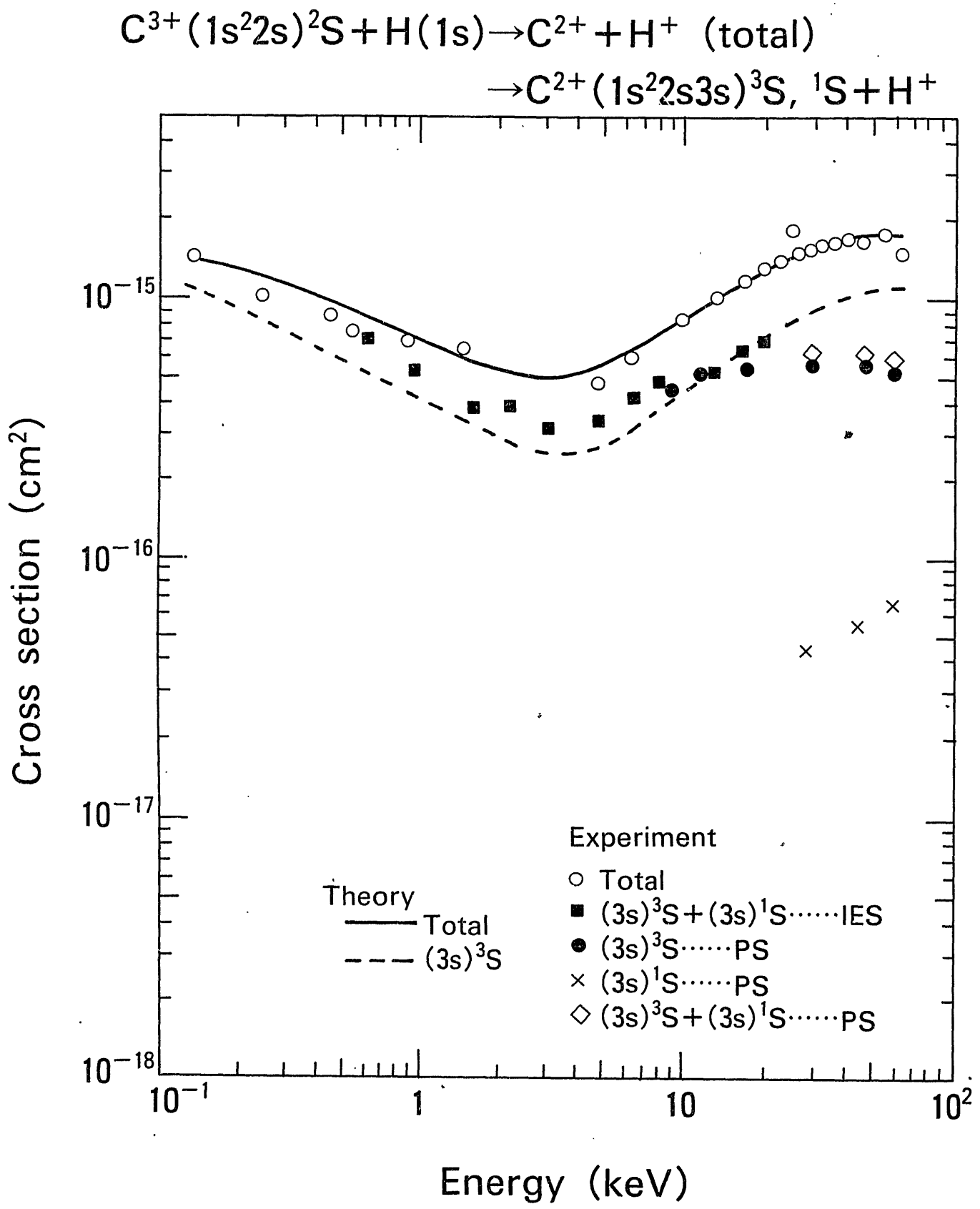

Fig.1 The cross sections of electron capture for $C^{3+}(1s^22s)^2S + H(1s) \rightarrow C^{2+} + H^+$ (total) and $C^{2+}(1s^22s3s)^3S$ and ^1S states.

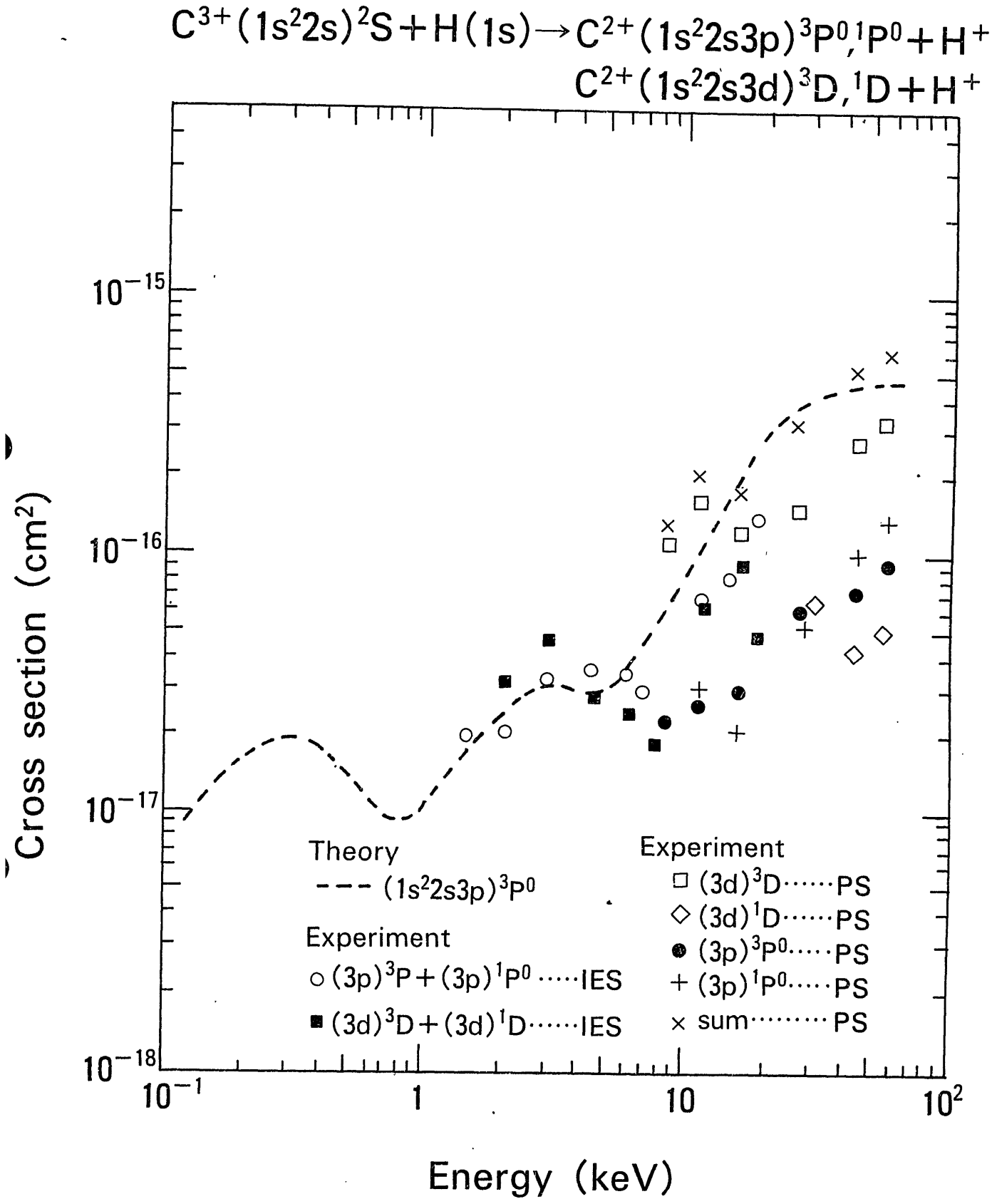

Fig.2 The cross sections of electron capture for $C^{3+}(1s^22s)^2S + H(1s) \rightarrow C^{2+}(1s^22s3p)^3P$ and ^1P, $C^{2+}(1s^22s3d)^3D$ and ^1D states.

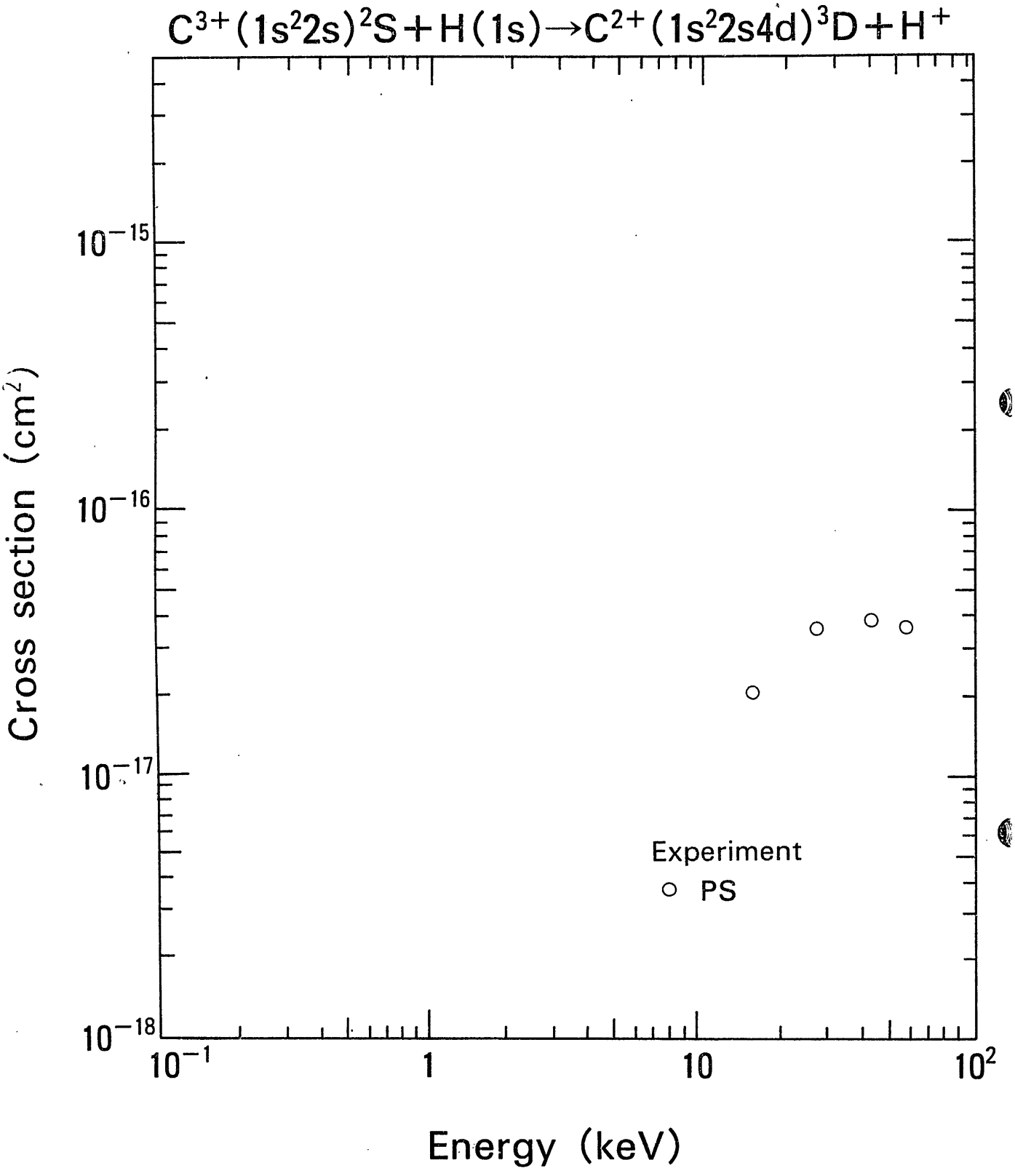

Fig.3 The cross sections of electron capture for $C^{3+}(1s^22s)^2S + H(1s) \rightarrow C^{2+}(1s^22s4d)^3D$ state.

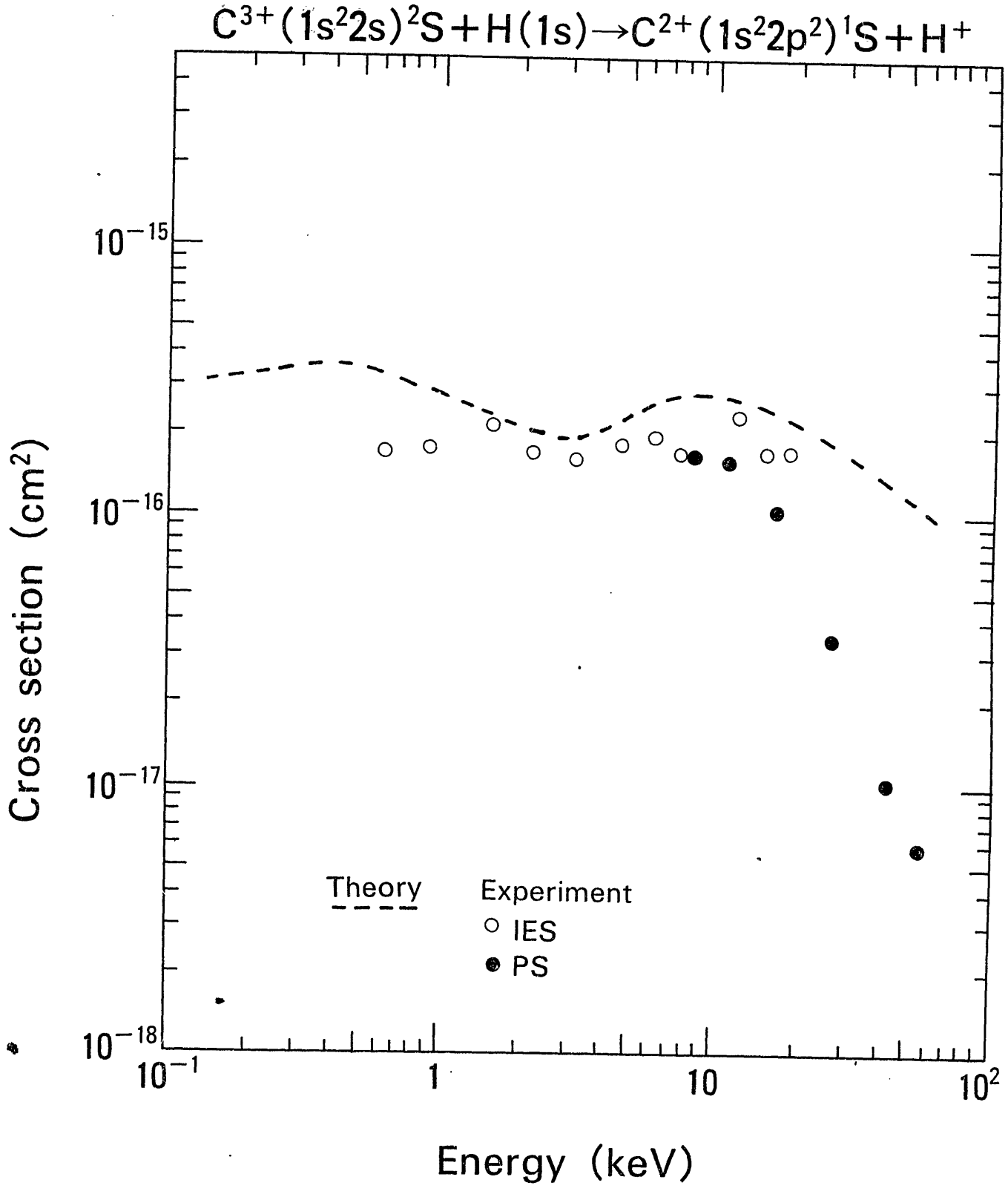

Fig.4 The cross sections of electron capture for $C^{3+}(1s^22s)^2S + H(1s) \rightarrow C^{2+}(1s^22p^2)^1S$ state.

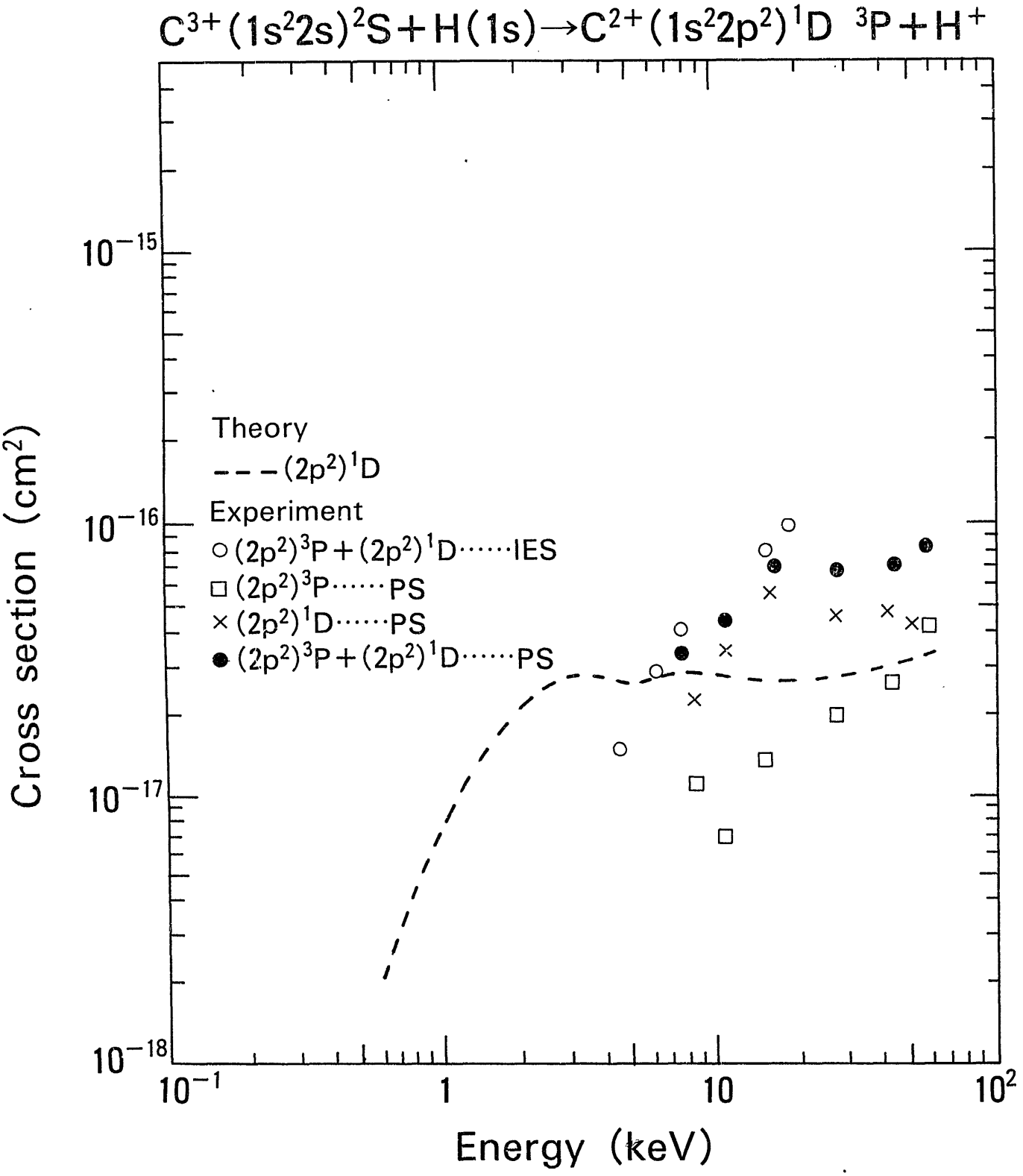

Fig.5 The cross sections of electron capture for $C^{3+}(1s^22s)^2S + H(1s) \rightarrow C^{2+}(1s^22p^2)^1D$ and ^3P states.

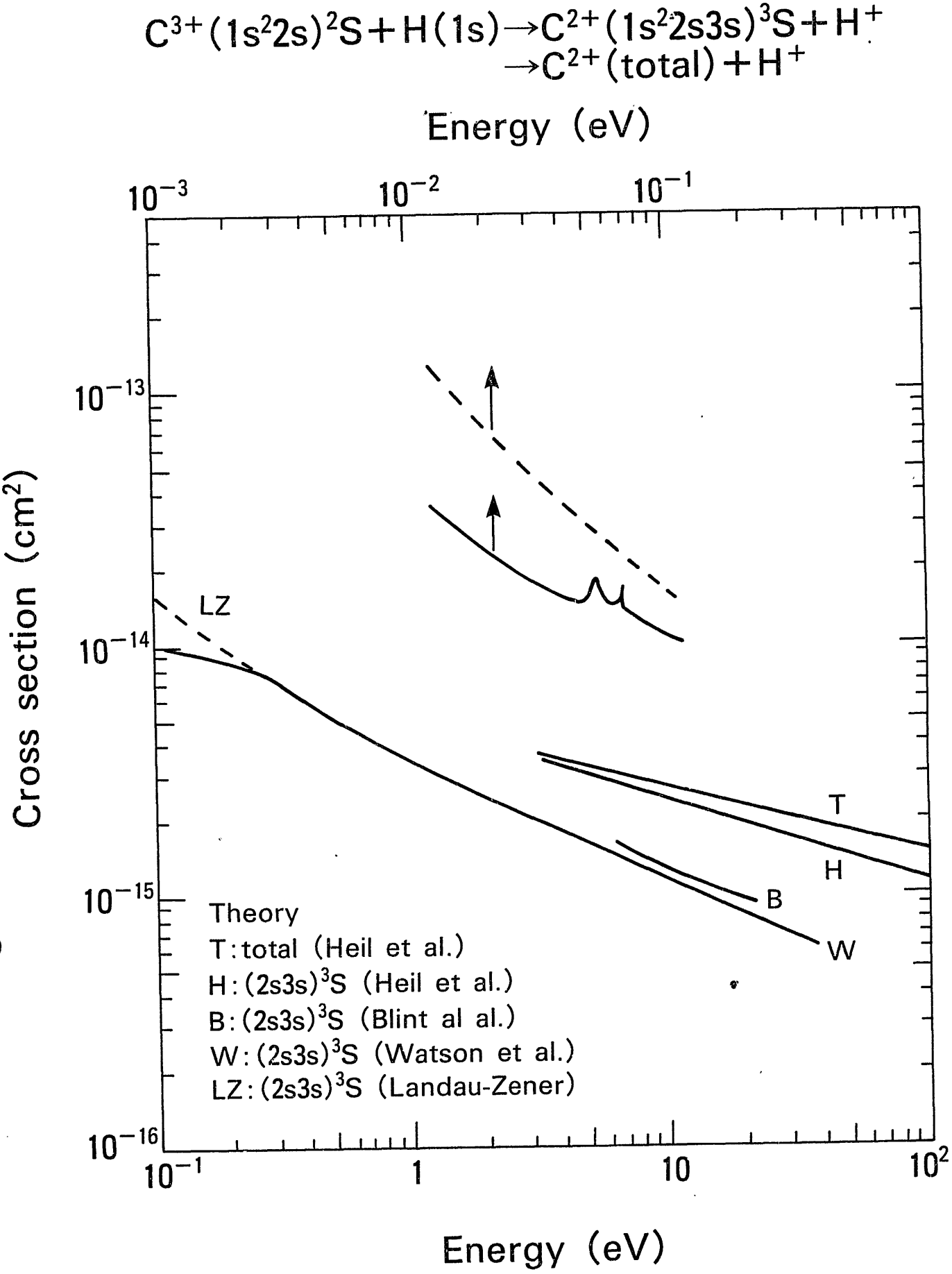

Fig.6 The cross sections of electron capture for $C^{3+}(1s^2 2s)^2S + H(1s) \rightarrow C^{2+} + H^+$ (total) and $C^{2+}(1s^2 2s3s)^3S$ state at lower energies.

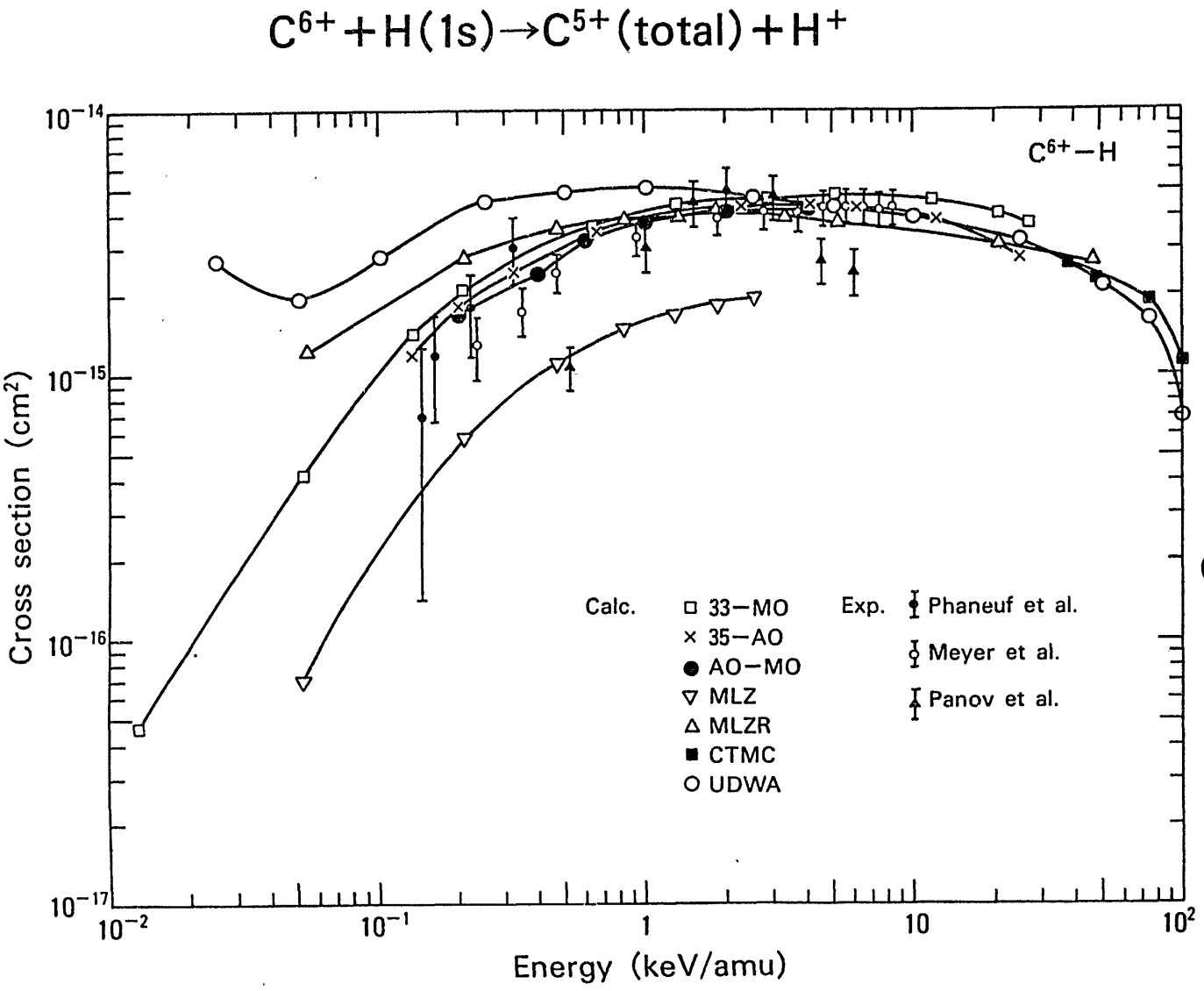

Fig.7. Total electron capture cross sections in C^{6+} + H collisions. The calculated results, MO, AO, AO-MO, MLZ, MLZR, CTMC, and UDWA, represent the results of close coupling method with 33-molecular states[11], close coupling method with 35-atomic states[12], atomic state-molecular state matching method[13], multichannel Landau-Zener method[14], multichannel Landau-Zener method with rotational transition[15], classical trajectory Monte Carlo method[16] and unitarized distored-wave method[17], respectively. Experimental results represent the data of Phaneuf et al.[18], Panov et al.[19] and Meyer et al.[20], respectively.

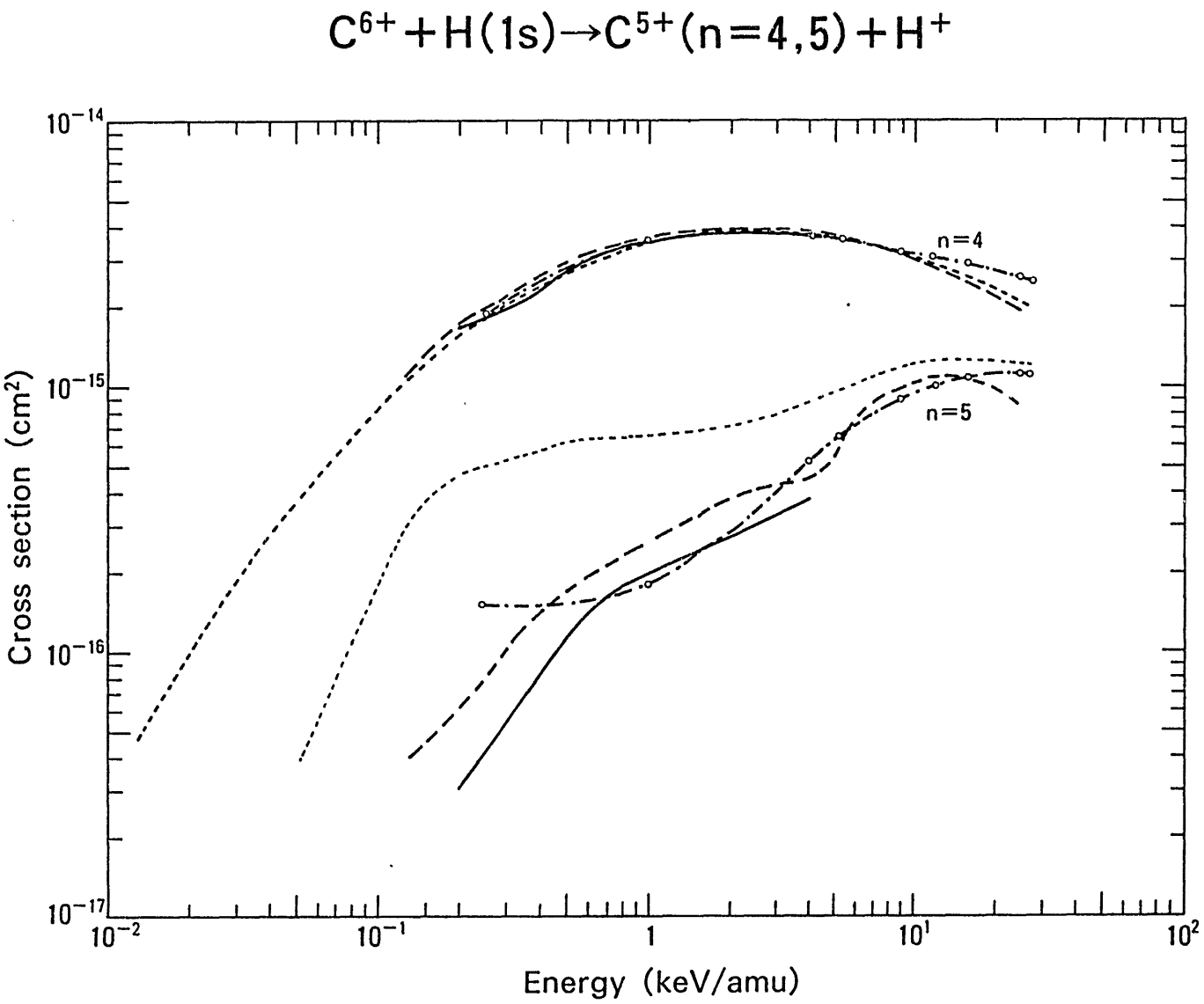

Fig.8. Partial cross sections for transfer into n = 4 and 5 states of C^{5+} ions. Results of MO, AO, AO-MO and small basis MO are shown in dotted, dashed, solid and dashed-dotted lines.

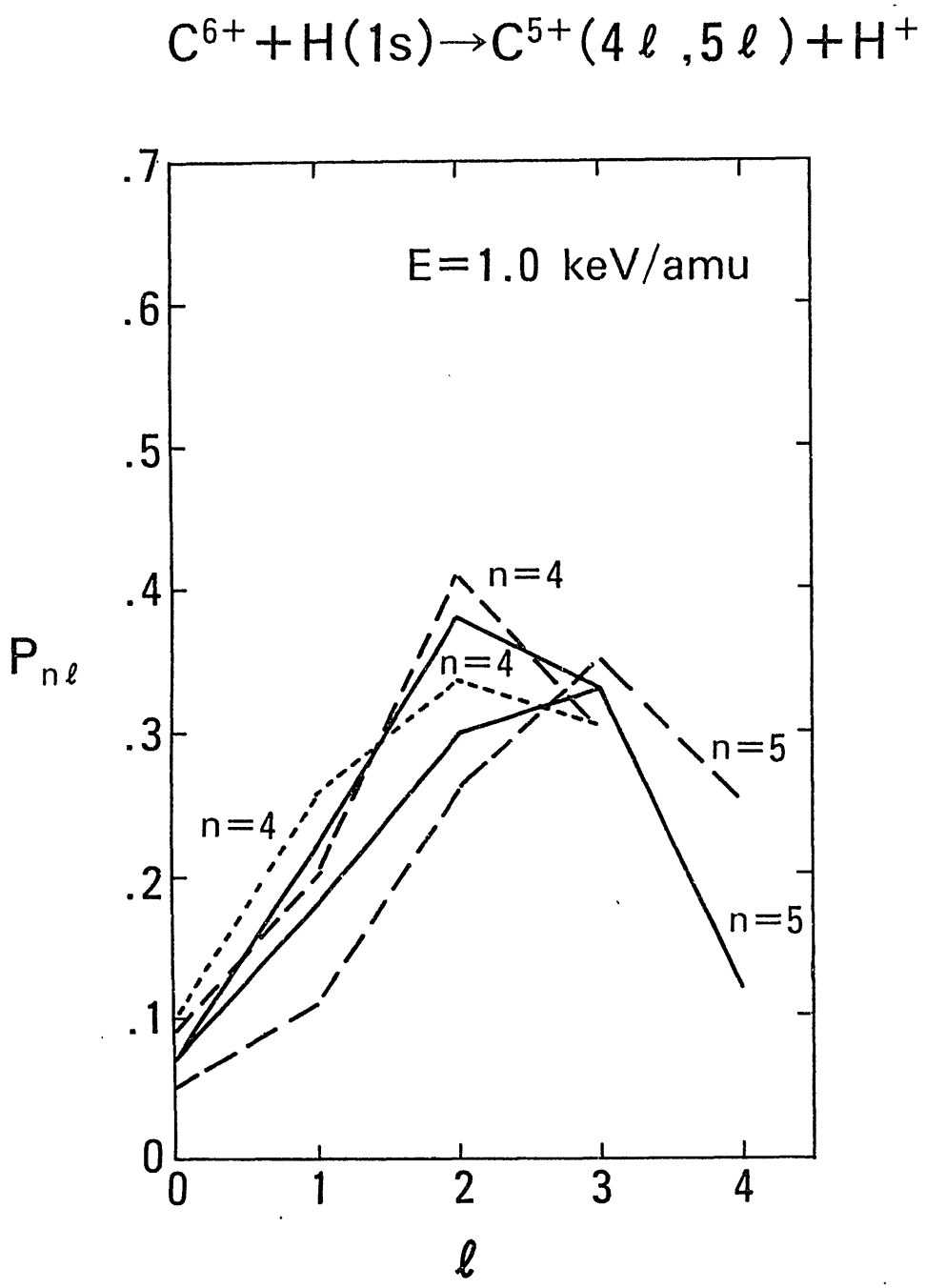

Fig.9(a) Relative population of specific ℓ-sublevels in the electron capture collisions $C^{6+} + H \rightarrow C^{5+}$ (n, ℓ) + H^{+} within the n = 4 and 5 manifolds at the incident energy E = 1.0 keV/amu. The solid, dashed and dotted lines represent the results of AO[12], AO-MO[13] and 11 molecular states with intershell mixing by Salin[23], respectively.

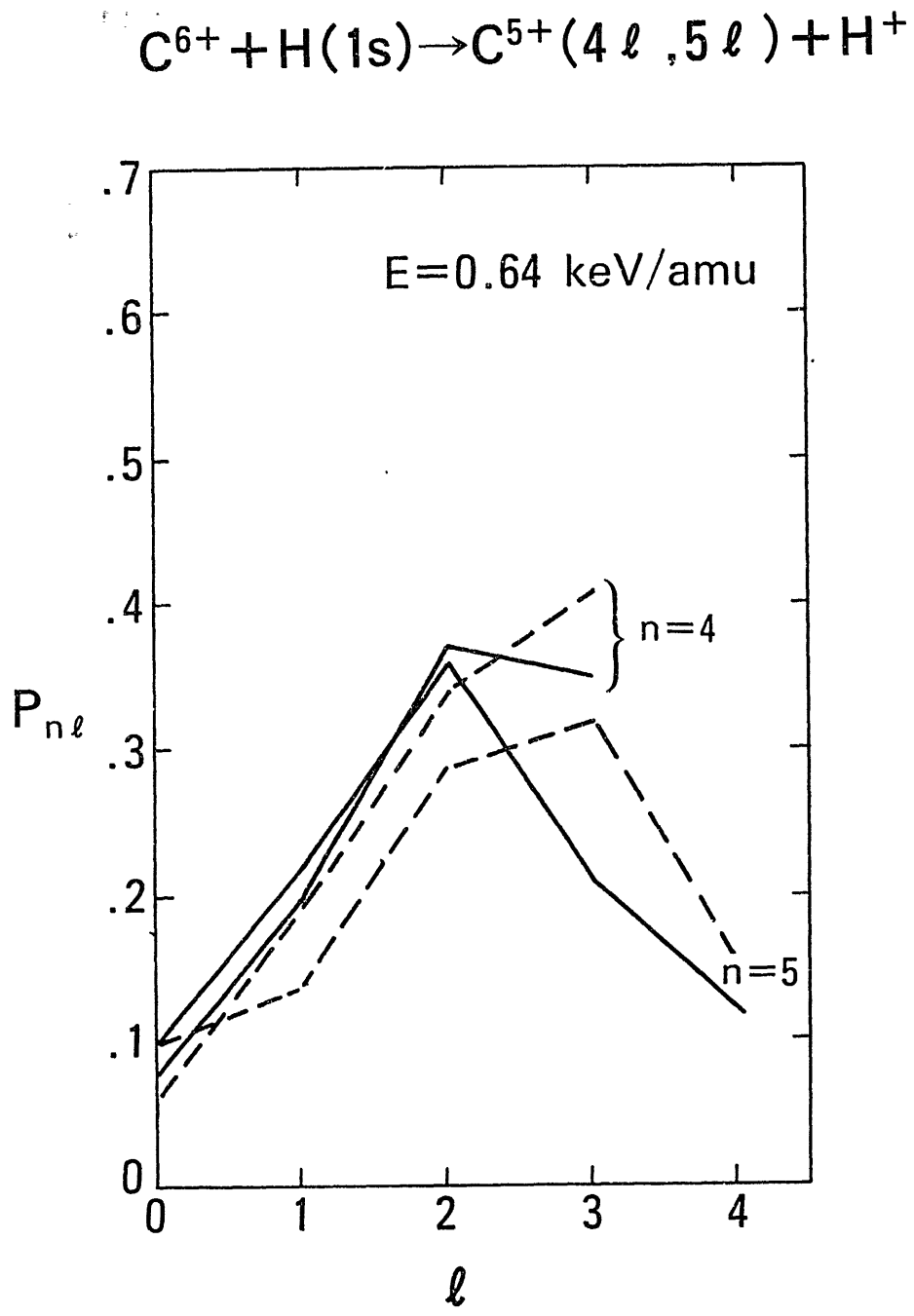

Fig.9(b) Relative population of specific ℓ-substates in the electron capture collisions $C^{6+} + H \rightarrow C^{5+}(n, \ell) + H^{+}$ within the n = 4 and 5 manifolds at the incident energy E = 0.64 keV/amu. The solid and dashed lines represent the results of AO[12] and MO[11], respectively.

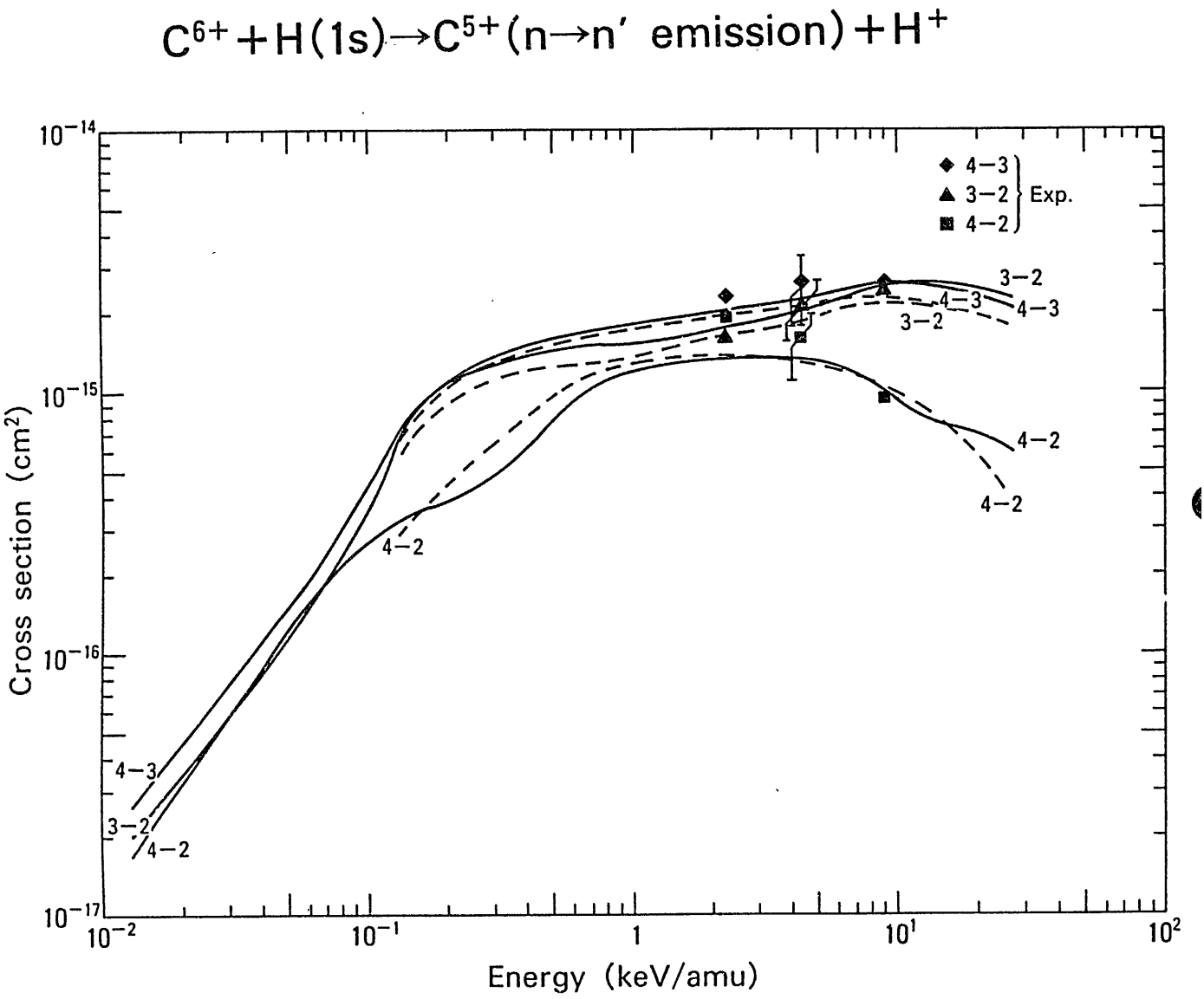

Fig.10(a) Line-emission cross sections $\sigma_{em}(n\text{-}n')$ of the $C^{5+}(n, \ell)$ ion as a function of the impact energy. Error bars indicate total uncertainties. Experimental results are by Dijkkamp et al.[10]. Solid and dashed lines represent the results by MO and AO, respectively.

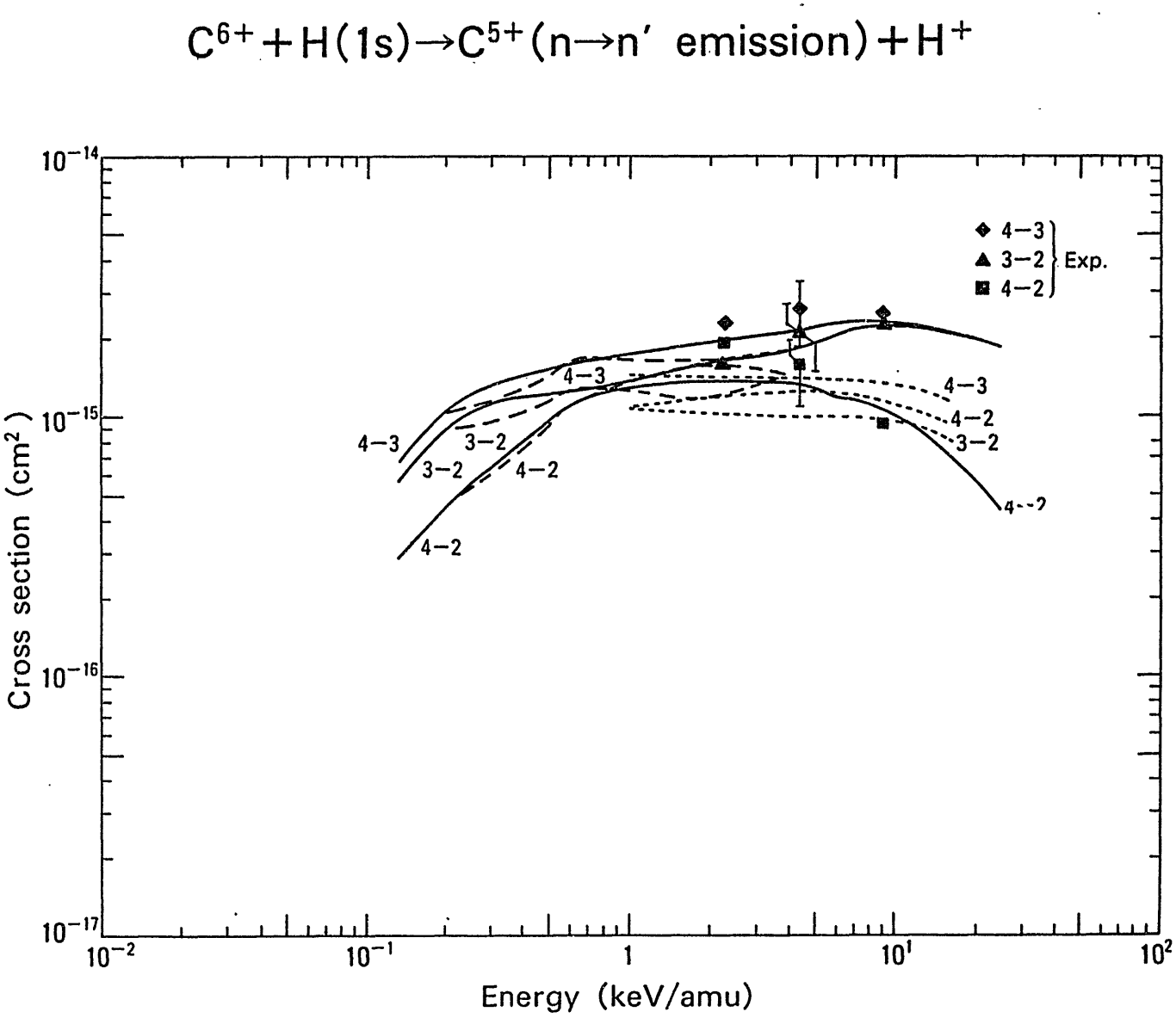

Fig.10(b) Line-emission cross sections $\sigma_{em}(n\text{-}n')$ of the $C^{5+}(n, \ell)$ ion as a function of the impact energy. Error bars indicate total uncertainties. Experimental results are by Dijkkamp et al.[10] Solid, dashed and dotted lines represent the results by AO[12], AO-MO[13] and Salin[23], respectively.

7. Concluding remarks

In the present work we have outlined some aspects of various theories for the electron capture of multiply charged ions in collisions with neutral atoms and discussed their limitation of validity. Some are relatively easily handled and expressed in analytical forms but they can not produce properly the behaviours such as the energy dependence of the cross sections, in particular the partial cross sections for (n, ℓ) distribution, even though total cross sections are compared favorably with experimental data. Even sophisticated, time-consuming calculations for simple collision systems involving atomic hydrogens are not always in good agreement with other calculations and limited experimental data though their predictions for dominant (n, ℓ) distributions generally agree with each other. Thus we are a bit uncertain if such sophisticated calculations as multichannel close coupling method provide reliable cross sections for somewhat complicated collision systems involving partially ionized ions and multi-electron targets. One of the reasons of these complications is due to the fact that reliable experimental data for (n, ℓ) distributions are only a few, though most of the measurements for total cross sections of the electron capture have been found to be in agreement with such calculations. Those given in section 6 are a few examples which have been investigated relatively well from both theory and experiment using different techniques. It is very clear from the present work that reliable and systematic measurements of the cross sections should be made in order to investigate and compare with theories. It should be emphasized, as mentioned already, that the reliable data for (n, ℓ) distributions are urgently required in many applications such as in use for diagnostics of high temperature plasmas as well as in rigorous test of the theories.

LIST OF IPPJ-AM REPORTS

IPPJ-AM-1* "Cross Sections for Charge Transfer of Hydrogen Beams in Gases and Vapors in the Energy Range 10 eV–10 keV"
H. Tawara (1977) [Published in Atomic Data and Nuclear Data Tables 22, 491 (1978)]

IPPJ-AM-2* "Ionization and Excitation of Ions by Electron Impact –Review of Empirical Formulae–"
T. Kato (1977)

IPPJ-AM-3 "Grotrian Diagrams of Highly Ionized Iron FeVIII-FeXXVI"
K. Mori, M. Otsuka and T. Kato (1977) [Published in Atomic Data and Nuclear Data Tables 23, 196 (1979)]

IPPJ-AM-4 "Atomic Processes in Hot Plasmas and X-Ray Emission"
T. Kato (1978)

IPPJ-AM-5* "Charge Transfer between a Proton and a Heavy Metal Atom"
S. Hiraide, Y. Kigoshi and M. Matsuzawa (1978)

IPPJ-AM-6* "Free-Free Transition in a Plasma –Review of Cross Sections and Spectra–"
T. Kato and H. Narumi (1978)

IPPJ-AM-7* "Bibliography on Electron Collisions with Atomic Positive Ions: 1940 Through 1977"
K. Takayanagi and T. Iwai (1978)

IPPJ-AM-8 "Semi-Empirical Cross Sections and Rate Coefficients for Excitation and Ionization by Electron Collision and Photoionization of Helium"
T. Fujimoto (1978)

IPPJ-AM-9 "Charge Changing Cross Sections for Heavy-Particle Collisions in the Energy Range from 0.1 eV to 10 MeV I. Incidence of He, Li, Be, B and Their Ions"
Kazuhiko Okuno (1978)

IPPJ-AM-10 "Charge Changing Cross Sections for Heavy-Particle Collisions in the Energy Range from 0.1 eV to 10 MeV II. Incidence of C, N, O and Their Ions"
Kazuhiko Okuno (1978)

IPPJ-AM-11 "Charge Changing Cross Sections for Heavy-Particle Collisions in the Energy Range from 0.1 eV to 10 MeV III. Incidence of F, Ne, Na and Their Ions"
Kazuhiko Okuno (1978)

IPPJ-AM-12* "Electron Impact Excitation of Positive Ions Calculated in the Coulomb-Born Approximation –A Data List and Comparative Survey–"
S. Nakazaki and T. Hashino (1979)

IPPJ-AM-13 "Atomic Processes in Fusion Plasmas – Proceedings of the Nagoya Seminar on Atomic Processes in Fusion Plasmas Sept. 5-7, 1979"
Ed. by Y. Itikawa and T. Kato (1979)

IPPJ-AM-14 "Energy Dependence of Sputtering Yields of Monatomic Solids"
N. Matsunami, Y. Yamamura, Y. Itikawa, N. Itoh, Y. Kazumata, S. Miyagawa, K. Morita and R. Shimizu (1980)

IPPJ-AM-15 "Cross Sections for Charge Transfer Collisions Involving Hydrogen Atoms"
Y. Kaneko, T. Arikawa, Y. Itikawa, T. Iwai, T. Kato, M. Matsuzawa, Y. Nakai, K. Okubo, H. Ryufuku, H. Tawara and T. Watanabe (1980)

IPPJ-AM-16 "Two-Centre Coulomb Phaseshifts and Radial Functions"
H. Nakamura and H. Takagi (1980)

IPPJ-AM-17 "Empirical Formulas for Ionization Cross Section of Atomic Ions for Electron Collisions –Critical Review with Compilation of Experimental Data–"
Y. Itikawa and T. Kato (1981)

IPPJ-AM-18 "Data on the Backscattering Coefficients of Light Ions from Solids"
T. Tabata, R. Ito, Y. Itikawa, N. Itoh and K. Morita (1981) [Published in Atomic Data and Nuclear Data Tables 28, 493 (1983)]

IPPJ-AM-19 "Recommended Values of Transport Cross Sections for Elastic Collision and Total Collision Cross Section for Eiectrons in Atomic and Molecular Gases"
M. Hayashi (1981)

IPPJ-AM-20 "Electron Capture and Loss Cross Sections for Collisions between Heavy Ions and Hydrogen Molecules"
Y. Kaneko, Y. Itikawa, T. Iwai, T. Kato, Y. Nakai, K. Okuno and H. Tawara (1981)

IPPJ-AM-21 "Surface Data for Fusion Devices – Proceedings of the U.S–Japan Workshop on Surface Data Review Dec. 14-18, 1981"
Ed. by N. Itoh and E.W. Thomas (1982)

IPPJ-AM-22 "Desorption and Related Phenomena Relevant to Fusion Devices"
Ed. by A. Koma (1982)

IPPJ-AM-23 "Dielectronic Recombination of Hydrogenic Ions"
T. Fujimoto, T. Kato and Y. Nakamura (1982)

IPPJ-AM-24 "Bibliography on Electron Collisions with Atomic Positive Ions: 1978 Through 1982 (Supplement to IPPJ-AM-7)"
Y. Itikawa (1982) [Published in Atomic Data and Nuclear Data Tables 31, 215 (1984)]

IPPJ-AM-25 "Bibliography on Ionization and Charge Transfer Processes in Ion-Ion Collision"
H. Tawara (1983)

IPPJ-AM-26 "Angular Dependence of Sputtering Yields of Monatomic Solids"
Y. Yamamura, Y. Itikawa and N. Itoh (1983)

IPPJ-AM-27 "Recommended Data on Excitation of Carbon and Oxygen Ions by Electron Collisions"
Y. Itikawa, S. Hara, T. Kato, S. Nakazaki, M.S. Pindzola and D.H. Crandall (1983) [Published in Atomic Data and Nuclear Data Tables 33, 149 (1985)]

IPPJ-AM-28 "Electron Capture and Loss Cross Sections for Collisions Between Heavy Ions and Hydrogen Molecules (Up-dated version of IPPJ-AM-20)
H. Tawara, T. Kato and Y. Nakai (1983) [Published in Atomic Data and Nuclear Data Tables 32, 235 (1985)]

IPPJ-AM-29 "Bibliography on Atomic Processes in Hot Dense Plasmas"
T. Kato, J. Hama, T. Kagawa, S. Karashima, N. Miyanaga, H. Tawara, N. Yamaguchi, K. Yamamoto and K. Yonei (1983)

IPPJ-AM-30 "Cross Sections for Charge Transfers of Highly Ionized Ions in Hydrogen Atoms (Up-dated version of IPPJ-AM-15)"
H. Tawara, T. Kato and Y. Nakai (1983) [Published in Atomic Data and Nuclear Data Tables 32, 235 (1985)]

IPPJ-AM-31 "Atomic Processes in Hot Dense Plasmas"
T. Kagawa, T. Kato, T. Watanabe and S. Karashima (1983)

IPPJ-AM-32 "Energy Dependence of the Yields of Ion-Induced Sputtering of Monatomic Solids"
N. Matsunami, Y. Yamamura, Y. Itikawa, N. Itoh, Y. Kazumata, S. Miyagawa, K. Morita, R. Shimizu and H. Tawara (1983) [Published in Atomic Data and Nuclear Data Tables 31, 1 (1984)]

IPPJ-AM-33 "Proceedings on Symposium on Atomic Collision Data for Diagnostics and Modelling of Fusion Plasmas, Aug. 29 – 30, 1983"
Ed. by H. Tawara (1983)

IPPJ-AM-34 "Dependence of the Backscattering Coefficients of Light Ions upon Angle of Incidence"
T. Tabata, R. Ito, Y. Itikawa, N. Itoh, K. Morita and H. Tawara (1984)

IPPJ-AM-35 "Proceedings of Workshop on Synergistic Effects in Surface Phenomena Related to Plasma-Wall Interactions, May 21 – 23, 1984"
Ed. by N. Itoh, K. Kamada and H. Tawara (1984) [Published in Radiation Effects 89, 1 (1985)]

IPPJ-AM-36 "Equilibrium Charge State Distributions of Ions ($Z_1 \geqq 4$) after Passage through Foils – Compilation of Data after 1972"
K. Shima, T. Mikumo and H. Tawara (1985) [Published in Atomic Data and Nuclear Data Tables 34, 357 (1986)]

IPPJ-AM-37 "Ionization Cross Sections of Atoms and Ions by Electron Impact"
H. Tawara, T. Kato and M. Ohnishi (1985) [Published in Atomic Data and Nuclear Data Tables 36, 167 (1987)]

IPPJ-AM-38 "Rate Coefficients for the Electron-Impact Excitations of C-like Ions"
Y. Itikawa (1985)

IPPJ-AM-39 "Proceedings of the Japan-U.S. Workshop on Impurity and Particle Control, Theory and Modeling, Mar. 12 – 16, 1984"
Ed. by T. Kawamura (1985)

IPPJ-AM-40 "Low-Energy Sputterings with the Monte Carlo Program ACAT"
Y. Yamamura and Y. Mizuno (1985)

IPPJ-AM-41 "Data on the Backscattering Coefficients of Light Ions from Solids (a Revision)"
R. Ito, T. Tabata, N. Itoh, K. Morita, T. Kato and H. Tawara (1985)

IPPJ-AM-42 "Stopping Power Theories for Charged Particles in Inertial Confinement Fusion Plasmas (Emphasis on Hot and Dense Matters)"
S. Karashima, T. Watanabe, T. Kato and H. Tawara (1985)

IPPJ-AM-43 "The Collected Papers of Nice Project/IPP, Nagoya"
Ed. by H. Tawara (1985)

IPPJ-AM-44 "Tokamak Plasma Modelling and Atomic Processes"
Ed. by T. Kawamura (1986)

IPPJ-AM-45 Bibliography of Electron Transfer in Ion-Atom Collisions
H. Tawara, N. Shimakura, N. Toshima and T. Watanabe (1986)

IPPJ-AM-46 "Atomic Data Involving Hydrogens Relevant to Edge Plasmas"
H. Tawara, Y. Itikawa, Y. Itoh, T. Kato, H. Nishimura, S. Ohtani, H. Takagi, K. Takayanagi and M. Yoshino (1986)

IPPJ-AM-47 "Resonance Effects in Electron-Ion Collisions"
Ed. by H. Tawara and G. H. Dunn (1986)

IPPJ-AM-48 "Dynamic Processes of Highly Charged Ions (Proceedings)"
Ed. by Y. Kanai and S. Ohtani (1986)

IPPJ-AM-49 "Wavelengths of K X-Rays of Iron Ions"
T. Kato, S. Morita and H. Tawara (1987)

IPPJ-AM-50 "Proceedings of the Japan-U.S. Workshop P-92 on Plasma Material Interaction/High Heat Flux Data Needs for the Next Step Ignition and Steady State Devices, Jan. 26 – 30, 1987"
Ed. by A. Miyahara and K. L. Wilson (1987)

IPPJ-AM-51 "High Heat Flux Experiments on C-C Composite Materials by Hydrogen Beam at the 10MW Neutral Beam Injection Test Stand of the IPP Nagoya"
H. Bolt, A. Miyahara, T. Kuroda, O. Kaneko, Y. Kubota, Y. Oka and K. Sakurai (1987)

IPPJ-AM-52 "Energy Dependence of Ion-Induced Sputtering Yields of Monatomic Solids in the Low Energy Region"
N. Matsunami, Y. Yamamura, N. Itoh, H. Tawara and T. Kawamura (1987)

IPPJ-AM-53 "Data Base on the High Heat Flux Behaviour of Metals and Carbon Materials for Plasma Facing Components -- Experiments at the 10 MW Neutral Beam Injection Test Stand of the IPP Nagoya"
H. Bolt, C. D. Croessmann, A. Miyahara, T. Kuroda and Y. Oka (1987)

IPPJ-AM-54 "Final (n, ℓ) State-Resolved Electron Capture by Multiply Charged Ions from Neutral Atoms"
N. Shimakura, N. Toshima, T. Watanabe and H. Tawara (1987)

Available upon request to Research Information Center, Institute of Plasma Physics, Nagoya University, Nagoya 464, Japan, except for the reports noted with*.